Centro de Investigación en Matemáticas, A.C.

CIMAT

The Boundary Element Method with Application to Transport in Heterogeneous Porous Media Problems

T E S I S

a mi Madre

Aknowledgements

To my Mother and my brother, that had been my help and support, at least, to put me in this place and moment.

To my advisor Francisco Solis, for backing me up through this year, for the confidence and effort on my behalf. Sincerely, thank you.

To my professors, Adrian Espinola, Silvia Jeréz and Ignacio Barradas, that made me understand the beauty of mathematics through the eyes of true understanding. A special thanks to a special friend: Lawrence Nash, whom helped me to realize that I can construct everything that I can imagine.

To my friends and colleagues, which made this trip not just possible, but exhilarating. Thank you from the bottom of my heart.

To CIMAT and CONACyT, that brought the resources that made possible for me to develop my studies and the research that concluded in this thesis.

To everyone that have joined my life, and the people that still remain by my side. Thanks to you all.

Quand tu veux construire un bateau, ne commence pas par rassembler du bois, couper des planches et distribuer du travail, mais reveille au sein des hommes le desir de la mer grande et large.

-Antoine de Saint-Exupéry-

Summary

The Boundary Element Method (BEM) is a numerical method for solving partial differential equations governing boundary value problems. The solution to a boundary value problem is usually expressed as a function of the whole domain. The BEM, however, transforms the nature of this solution to from a full-domain-dependent-solution to a boundary-dependent solution; allowing a low computational method to solve boundary value problems. The method relies on the integral representation of the partial differential equations governing the problem. The boundary integral equations, from which the problem is solved, arise as a direct consequence of the properties of Green's functions. Using these integral representations we set a system of linear algebraic equations which is solved to obtain the solution to the problem in a particular set over the problem's domain.

Transport processes in porous media could be described by a dispersive-convective transport equation. Studying this kind of phenomena gives place to boundary value problems governed by this equation, where the dispersive coefficient results as a time dependent function. The correct interpretation of the model relies on a precise approximation to the problem's solution. In this sense, the Boundary Element Method provide us with a tool to avoid possible problems during operations over porous media.

In this thesis we will develop a numerical tool to solve a general class of boundary value problems, flow behaviour through porous media among them. For doing so, we will discuss the development of various class of boundary element methods: first and second order boundary element methods with polynomial and thin plate spline approximations are discussed. Also, the precision of the method is evaluated by comparing the numerical results with the exact solution for some problems. Once the method is established, we apply it to solve a dispersive-convective transport equation to study the behaviour of a flow process trough porous media.

Contents

Introduction

The Boundary Element Method (BEM) is a numerical tool for solving boundary value problems. The method explicitly develops the solution to the partial equations governing the boundary value problem as a boundary integral equation which can be solved numerically. Using these integral representations we set a system of linear algebraic equations which is solved to obtain the solution to the problem.

Transport processes in porous media could be described by a dispersive-convective transport equation. Studying this kind of phenomena gives place to boundary value problems, where the dispersive coefficient results as a time dependent function. Poor predictions of the model could give bad predictions related with field operations. The correct interpretation of the model relies on a precise approximation to the problem's solution, proven that the solution is not available. In this sense, the Boundary Element Method provide us with a tool to correctly analyse data from the mathematical model, predicting possible problems during operations over porous media.

Thesis Overview

This document presents the clear development and implementation of a numerical tool. The careful discussion of the algorithm and the comparative study between variations of boundary element methods, which has not been formally discussed in literature, sets a starting point for future work. The method discussed trough this thesis can be easily extended in different directions, strengthening the method to solve more complex problems with relatively ease.

During this thesis we will establish the fundamental theory behind the application of boundary element methods. Once this is set, a few examples will be discussed to end with the resolution of a problem that surges from hydrocarbon recovery in oil reservoirs. The document is divided in three chapters, and a final section to discuss conclusions and future work, each one containing one of the following:

Chapter 1: The Boundary Element Method

Here, using Green's third identity, we establish the harmonic solution to a boundary value problem in the form of an integral equation. This serves as the nucleus of boundary element methods. Once the integral equation is defined over the problem's boundary, giving form to discrete the boundary value representation, we use it to approximate the missing values of the potential, or its normal derivative. With a full knowledge of the boundary values the solution is completed. In this chapter we develop the procedure to apply Boundary Element Methods to solve the Laplace equation defined on connected compact sets of $\mathbb{R}^2$.

Chapter 2: BEM for Poisson's Equation

Here we extend the theoretical basis of boundary element methods to handle the solution to equations more complex than Laplace's, particularly Poisson's equation. We first study the arise of domain integrals at boundary representations for models with non-homogenous sources. Then, using Green's second identity, and assuming the knowledge of a particular solution to Poisson's equation, we get rid of the domain integrals. This leads to a boundary representation that depends on the values of the function and the particular solution at the domain's boundary. As sometimes is difficult to know the

particular solution, a dual reciprocity principle is used to approximate it in a series of known functions. This defines de dual reciprocity boundary element method, which is extended to consider wider problems. In this chapter we construct a boundary element method for solving problems where potential, advection, and time dependent terms arise.

Chapter 3: Transport in Porous Media

Here we present a model published in the literature by Numbere and Erkal, 1998, that describes accurately anomalous anisototropic transport processes in porous media. This results in an usual advective-difusive transport equation with a time dependent dispersion coefficient. The model is introduced as a reduction from a stochastic process that follows from a geostatical framework. Once the model is presented, a dual reciprocity method is stated to solve the equation. At the end of the chapter we present some numerical results and a brief discussion about them.

Chapter 1

The Boundary Element Method

The Boundary Element Method is a numerical method for solving partial differential equations encountered in the math-physics and engineering. Examples include Laplace's equation, Helmholtz's equation, the convection diffusion equation, and the equations of potential and viscous flow. In principle, any differential equation can be resolved with the BEM. However, this method is efficient, and thus appropriate, for linear, elliptic, and homogeneous partial differential equations governing boundary-value problems in the absence of an homogeneous source.

The key idea behind the BEM is to express the solution of a partial differential equation in terms of boundary distributions. This process leads to an integral representation of the problem in terms of the problem's boundary values. Once the boundary distributions are fully determined, the solution to the problem at any point of the domain can be determined through direct evaluation, Pozrikidis [22].

In this chapter the basic formulation of the method for solving the Laplace equation is presented. In the first section of this chapter we will discuss the requirements that a problem has to accomplish so it can be solved using BEM. Then we establish the required background to develop the Boundary Element Method and stablish the general procedure to solve Laplace's equation. Next, the problem is posed in matrix form, explaining how the boundary element influence coefficients are obtained and the boundary conditions applied. The cases of constant an linear elements are discussed together. Finally, some numerical results are presented and discussed.

1.1 Boundary Element Methods Overview

A large amount physical phenomena occurring in nature can be described by differential equations and boundary conditions. In the solution to these boundary value problems we aim to determine a response to given boundary conditions. Analytical solutions to boundary value problems, *i.e* solutions that satisfy both the differential equations and the boundary conditions, can only be obtained for few problems with very simple assumptions. As an example, we may be interested in determining the response of a rock mass due to the excavation of a tunnel. Analytical solutions for this problem exist only if we consider the excavation circular tunnel in in a homogeneous rock mass, not the most realistic scenario for practical tunnelling. To be able to solve real life problems, we must revert very frequently to approximate solutions.

The term *Boundary Element Method* derives from the practice of discretizing the boundary of a solution domain into "boundary-elements" as a part of the resolution of the problem. In the case of a two-dimensional solution domain, the boundary is a planar line, and the boundary elements are straight segments, parabolas, circular arcs, or cubic segments.

The theoretical formulation and numerical methods related with the Boundary Element method can be applied to differential equations of the general form

$$L[u] = 0, \ \ \text{in} \ \ \Omega, \tag{1.1}$$

where $L[\cdot]$ is a differential operator satisfying the following properties, Pozrikidis [22]:

- The differential operator $L[\cdot]$ is elliptic.

- The differential equation is homogeneous.

- The differential equation is linear.

- The fundamental solution to the differential equation is available.

If we can assure that $L[\cdot]$ has the previous properties, then: the solution to (1.1) is determined exclusively by data specified around the boundary of Ω, a zero-solution follows from zero-valued boundary conditions, and the boundary integral equation for the problem is available.

The numerical method describes the solution $u(x_i)$ to the problem (1.1), for any interior point x_i in the problem's domain, as a function that depends only on the boundary values. To solve a problem using BEM the following approach is taken:

1. Develop an incomplete boundary representation for the solution to the boundary value problem.

2. State an integral equation to recover the unknown boundary values of the problem.

3. Solve numerically the boundary integral equation for the unknown boundary values.

4. Complete the solution of the problem as a boundary value representation.

1.2   BEM for Laplace's Equation

The Boundary Integral Representation

Consider that we are seeking the solution of a Laplace equation in a two-dimensional domain Figure 1.1,

$$\nabla^2 u = 0 \text{ in } \Omega, \tag{1.2}$$

with the following boundary conditions

1. "Essential" conditions of the type $u = \bar{u}$ on Γ_1.

2. "Natural" conditions such as $q := \dfrac{\partial u}{\partial n} = \bar{q}$ on Γ_2,

where n is the outward normal to the boundary $\Gamma = \Gamma_1 + \Gamma_2$, $\bar{u}$ and $\bar{q}$ are known functions.

The starting boundary integral equation required by the method can be deduced in a simple way considering Green's third identity. Let ψ and ϕ be scalar functions defined on some simply connected, bounded region $\Omega \subset \mathbb{R}^2$. Suppose that ψ is twice differentiable, and ϕ is once differentiable, then

$$(\phi\psi_x) = \phi_x\psi_x + \phi\psi_{xx}.$$
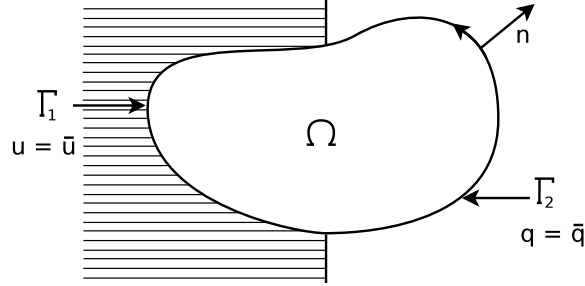
Figure 1.1: Bidimensional domain Ω for Laplace's equation.

The same is true for the derivative respect to y. Summing both derivatives leads to the following identity

$$\nabla \cdot (\phi \nabla \psi) = \nabla \phi \cdot \nabla \psi + \phi \nabla^2 \psi.$$

If we integrate over Ω and use the divergence theorem on the left side, then

$$\int_\Gamma \phi \frac{\partial \psi}{\partial n} d\Gamma = \iint_\Omega (\nabla \phi \cdot \nabla \psi) d\Omega + \iint_\Omega (\phi \nabla^2 \psi) d\Omega. \qquad (1.3)$$

This is *Green's first identity*, and it is valid for any solid region Ω, and any pair of functions ψ and ϕ that satisfy the differentiability conditions. Now, switching ψ and ϕ in (1.3)

$$\int_\Gamma \psi \frac{\partial \phi}{\partial n} d\Gamma = \iint_\Omega (\nabla \psi \cdot \nabla \phi) d\Omega + \iint_\Omega (\psi \nabla^2 \phi) d\Omega. \qquad (1.4)$$

If we subtract (1.4) from (1.3), then

$$\iint_\Omega \left(\phi \nabla^2 \psi - \psi \nabla^2 \phi \right) d\Omega = \int_\Gamma \left(\phi \frac{\partial \psi}{\partial n} - \psi \frac{\partial \phi}{\partial n} \right) d\Gamma. \qquad (1.5)$$

This is *Green's second identity* and it is valid for any solid region Ω, and for any pair of functions ψ and ϕ.

The fundamental solution $u_i^* = u^*(x, x_i)$, represents the field generated by a concentrated unit source acting at a point x_i. The effect of this source is propagated from x_i to infinity without any consideration of boundary conditions. This can be established as u_i^* satisfying the following equation,

$$\nabla^2 u_i^* + \delta_{x_i} = 0,$$

where δ_{x_i} stands for the Dirac delta distribution centered at x_i, which corresponds to the definition of the fundamental solution for Laplace's equation. It can be easily demonstrated, using the properties of the delta distribution, that if u is harmonic and $x_i \in \Omega$, then

$$\int_\Omega u(\nabla^2 u_i^*) = \int_\Omega u(-\delta_{x_i}) = -u_i,$$

where we take the nomenclature standard $u_i = u(x_i)$. Equating $\phi = u$, harmonic, and $\psi = u_i^*$ on Green's second identity (1.5) we get Green's third identity:

$$u_i = \int_\Gamma u_i^* q d\Gamma - \int_\Gamma q_i^* u d\Gamma, \tag{1.6}$$

where q_i^* corresponds to the normal derivative of the fundamental solution centred at x_i. This defines an integral equation for the solution to any harmonic function at the interior point x_i. The formalism of Green's third identity can be resumed in the following theorem:

Theorem 1.1 (Harmonic Interior Boundary Representation). Let $x_i \in \Omega$, where Ω is an open, simple connected region contained in $\mathbb{R}^2$ with boundary Γ, and let u be harmonic in Ω. Then $u(x_i)$ can be expressed as

$$u(x_i) = \int_\Gamma u^*(x, x_i) \frac{\partial u}{\partial n}(x) dx - \int_\Gamma u(x) \frac{\partial u^*}{\partial n}(x, x_i) dx \quad x_i \in \Omega \tag{1.7}$$

Where,

$$u^*(x, x_i) = -\frac{1}{2\pi} \ln|x - x_i|_2$$

is the fundamental solution to Laplace's operator, and

$$\frac{\partial u^*}{\partial n}(x, x_i) = -\frac{n \cdot (x - x_i)}{\|x - x_i\|_2^2}.$$

Equation (1.7) provides a solution to a harmonic function in terms of the boundary values and the boundary distribution of the normal derivative of the harmonic function. This is known as the a boundary-integral representation. To compute the value of u at a particular point x_i inside a selected control area, we simply evaluate the two boundary integrals on the right-hand side of (1.7).

The boundary value representation is the cornerstone of the boundary element method, and it is not exclusive for the solution to Laplace's Equation. The equation (1.7) can be easily extended to various elliptical operators governing a boundary value problem, if the fundamental solutions are available. Solutions to Helmholtz' equation and the stationary diffusive transport equation can be found at sections 2.2 and 2.3 from Pozrikidis [22]. This work will consider only the application of the equation presented in Theorem 1.1, a little discussion about further applications is considered for future work.

The Boundary Integral Equation

The integral equation (1.7) is valid for any point within the domain Ω. However, and as attractive as it could result, the Boundary Representation is not completely developed yet. Usually, the boundary data is not fully-available *a priori*. To recover the missing information of the problem we need to apply equation (1.7) on the boundary, and it is necessary to find out what happens when the point x_i is on Γ. The following approach is taken from Partridge, [18].

Lets return to the integral representation (1.7), and consider that the point x_i is on a smooth boundary. Suppose that the domain itself is augmented by a semicircle as shown in Figure 1.2, the extended boundary is represented as Γ_ε. The boundary point x_i is considered to be at the center
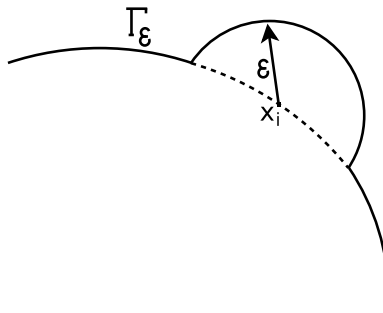

Figure 1.2: Extended boundary to evaluate (1.7) at a boundary point.

of the semicircle, and then the limit as the radius ε tends to zero is evaluated. The point will then become again a boundary point and the resulting expression will be the specialization of (1.7) for a point on Γ.

Evaluating the boundary representation (1.7) using the extended boundary Γ_ε leads to

$$u_i + \int_{\Gamma_\varepsilon} u q_i^* d\Gamma_\varepsilon = \int_{\Gamma_\varepsilon} q u_i^* d\Gamma_\varepsilon. \tag{1.8}$$

Careful examination for the integral term at the right side of (1.8) shows that it vanishes as $\varepsilon \to 0$,

$$\lim_{\varepsilon \to 0} \int_{\Gamma_\varepsilon} q u_i^* d\Gamma_\varepsilon = \lim_{\varepsilon \to 0} \int_{\Gamma_\varepsilon} -\frac{1}{2\pi} \ln \|x - x_i\|_2 \frac{\partial u}{\partial n}(x) dx = 0. \tag{1.9}$$

In other words, this term is a continuous integral when evaluated at the boundary. For the term at the left side we have

$$\lim_{\varepsilon \to 0} \int_{\Gamma_\varepsilon} u q_i^* d\Gamma_\varepsilon = \lim_{\varepsilon \to 0} \int_{\Gamma_\varepsilon} -u(x) \frac{\partial}{\partial n} \left(\ln \|x - x_i\|_2 \right) dx = -\frac{1}{2} u_i \tag{1.10}$$

This means that the integral has a discontinuity, or jump, on the boundary, and it produces what is called a free term. Finally, evaluating equation (1.7) at the boundary point x_i, using (1.9) and (1.10), leads to

Theorem 1.2 (Harmonic Boundary Representation). Let $x_i \in \Gamma$, where Γ is the smooth boundary of an open, simple connected region Ω contained in $\mathbb{R}^2$, and let u be harmonic in Ω. Then $u(x_i)$ can be expressed using the following integral equation

$$\frac{1}{2} u(x_i) + \int_\Gamma u(x) \frac{\partial u^*}{\partial n}(x, x_i) dx = \int_\Gamma u^*(x, x_i) \frac{\partial u}{\partial n}(x) dx \quad x_i \in \Gamma, \tag{1.11}$$

Where,

$$u^*(x, x_i) = -\frac{1}{2\pi} \ln|x - x_i|_2$$

is the fundamental solution to Laplace's operator, and

$$\frac{\partial u^*}{\partial n}(x, x_i) = -\frac{n \cdot (x - x_i)}{\|x - x_i\|_2^2}.$$

The integrals at equation (1.11) are calculated in the sense of Cauchy Principal Values. This is the boundary integral equation generally used as the starting point for the boundary element formulation. Now, the Boundary Element Method is based on the following observations, Pozrikidis [22]:

- Given the boundary distribution of the function u, equation (1.11) reduces to a *Fredholm integral equation of the first kind* for the normal derivative $q \equiv n \cdot \nabla u$. To show this more explicitly, we recast the integral equation as

$$\int_\Gamma u^*(x, x_i) q(x) dx = F(x_i), \qquad (1.12)$$

  where

$$F(x_i) = -\frac{1}{2} u(x_i) + \int_\Gamma u(x) \frac{\partial u^*}{\partial n}(x, x_i) dx$$

  is a known source term consisting of the boundary values of u and its distribution over the problem's boundary.

- Given the boundary distribution of the normal derivative $n \cdot \nabla u$, equation (1.11) reduces to a *Fredholm integral equation of the second kind* for the boundary distribution of u. To show this more explicitly, we recast the integral equation into the form

$$u(x_i) = 2 \int_\Gamma u(x) \frac{\partial u^*}{\partial n}(x, x_i) dx + \Phi(x_i) \qquad (1.13)$$

  where

$$\Phi(x_i) = -2 \int_\Gamma u^*(x, x_i) \frac{\partial u}{\partial n}(x) dx$$

  is a known source term consisting of the distribution of the normal derivative of u over the problems boundary.

The main goal of the Boundary Element Method is to generate numerical solutions to the integral equations (1.12) and (1.13). The numerical implementation of the boundary element collocation method, to be discussed in detail in the following section, involves the following steps:

1. Discretize the boundary into a collection of boundary elements, and approximate the boundary integrals with sums of integrals over the boundary elements.

2. Introduce approximations for the unknown function, u or q, over the individual boundary elements.

3. Apply the integral equation at collocation points located over the boundary elements to generate a number of linear algebraic equations equal to the number of unknowns.

4. Perform the integration over the boundary elements.

5. Solve the linear system for the coefficients involved in the approximation of the unknown function.

In performing and interpreting the results of a boundary-integral computation, it is important to have a good understanding of the existence and uniqueness of the solution. If the integral equation does not have a solution or if the solution is not unique, poorly conditioned or singular algebraic systems with erroneous solutions will arise.

The Discrete Integral Representation

The Boundary Element Method derives its name from the practice of describing the boundary of a solution with a collection of elementary geometrical units called boundary elements. In the case of Laplace's equation in two dimensions, the boundary elements are line segments with straight or curved shapes described in analytical form by methods of function interpolation and approximation in terms of element nodes, Pozrikidis [22].

A variety of boundary elements are available in two dimensions. Three popular choices are linear elements with straight shapes, circular arcs, and elements of cubic splines. For sake of simplicity, we will stablish the BEM using straight elements. Some work developed using cubic splines or circular arcs can be consulted at [22].

Figure 1.3 illustrates the discretization of a boundary into a collection of N straight elements defined by the element end-point vertex. The element labels increase in the counterclockwise direction around the boundary. Since the second end-point of an element is the first end-point of the next element, the collection of the N elements is defined by $N+1$ distinct (unique) points. If the boundary is closed, the first and last global nodes coincide, and the collection of the N elements is defined by N distinct vertices.

To describe the j-th element, Figure 1.4, we introduce the coordinates of the end-points $\mathbf{x}_j^0 = (x_j^0, y_j^0)$, $\mathbf{x}_j^l = (x_j^l, y_j^l)$, two interpolating functions ϕ^- and ϕ^+, and the dimensionless parameter ξ (S at Figure) ranging in the
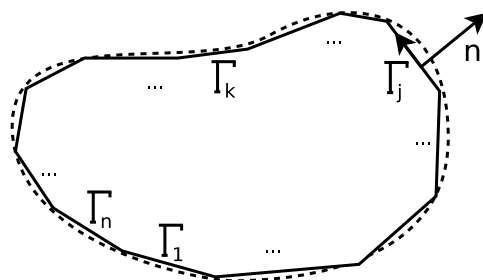
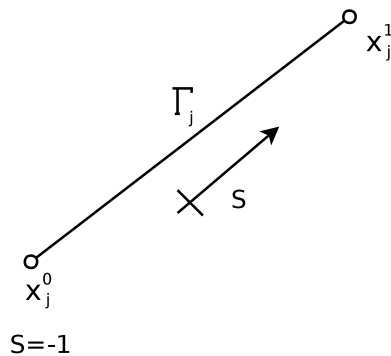Figure 1.3: Discrete boundary approximation.

Figure 1.4: Straight element parametrization.

interval $[-1, 1]$. Then, the coordinates of a point in the element are given by

$$
\begin{aligned}
x(\xi) &= x_j^0 \phi^-(\xi) + x_j^l \phi^+(\xi) \\
y(\xi) &= y_j^0 \phi^-(\xi) + y_j^l \phi^+(\xi).
\end{aligned}
\tag{1.14}
$$

Where,

$$
\begin{aligned}
\phi^+(\xi) &= \tfrac{1}{2}(1 + \xi), \\
\phi^-(\xi) &= \tfrac{1}{2}(1 - \xi).
\end{aligned}
\tag{1.15}
$$

As ξ increases from -1 to 1, the point $\mathbf{x}(\xi)$ moves from the first element end-point to the second element end-point.

Let us consider how expression (1.11) can be discretized to find the system of equations from which the boundary values can be found. Assume that the

boundary is divided into N segments as shown in Figure 1.3. The points where the unknown values are considered are called "nodes" and taken to be in the middle of each straight element for the so-called constant elements, Fig 1.5 (Left). We will later discuss the case of linear elements, *i.e.* those
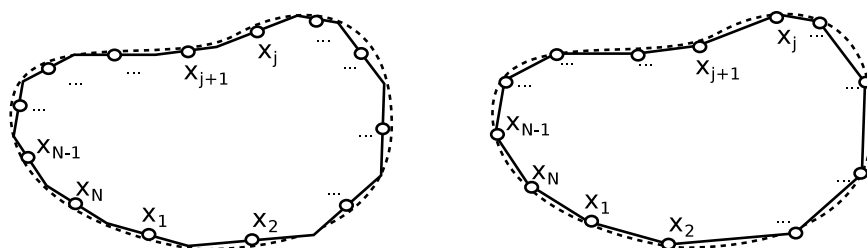

Figure 1.5: Constant element nodal distribution, Left; Linear element nodal distribution, Right

elements for which the nodes are at the extremes or ends. A boundary element method which considers constant approximations over each element is called 0-BEM from now on.

The boundary-integral representation (1.11) can now be discretized. To do so, lets take the procedure discussed by Patridge at [18]:

Evaluating at a given node $\mathbf{x}_i = (x_i, y_i)$, substituting the boundary by the boundary approximation follows

$$\frac{1}{2}u_i + \sum_{j=1}^{N} \int_{\Gamma_j} u q_i^* d\Gamma_j = \sum_{j=1}^{N} \int_{\Gamma_j} q u_i^* \Gamma_j.$$

In the case of the constant elements the values of u and its normal derivative q are assumed to be constant over each element and equal to the value at the mid-element node. The points at the extremes of the elements are used only for defining the geometry of the problem. Note that for this type of element the boundary is always smooth at the nodes as these are located at the center of the elements, hence the multiplier of u_i is always $\frac{1}{2}$.

The u and q values can thus be taken out of the integrals. They will be called u_j and q_j for element Γ_j. Hence,

$$\frac{1}{2}u_i + \sum_{j=1}^{N} u_j \int_{\Gamma_j} q_i^* d\Gamma_j = \sum_{j=1}^{N} q_j \int_{\Gamma_j} u_i^* \Gamma_j.$$

Notice that there are now two types of integrals to be carried out over each element,

$$\int_{\Gamma_j} q_i^* d\Gamma_j \quad \text{and} \quad \int_{\Gamma_j} u_i^* \Gamma_j.$$

These integrals relate the node $\mathbf{x}_i$, where the fundamental solution is applied, to the boundary element Γ_j. Because of this, their resulting values are sometimes called *influence coefficients*,

$$G_{ij} = G_j(\mathbf{x}_i) = \int_{\Gamma_j} u^*(\mathbf{x}, \mathbf{x}_i) d\mathbf{x}, \tag{1.16}$$

and

$$\overline{H}_{ij} = \overline{H}_j(\mathbf{x}_i) = \int_{\Gamma_j} \frac{\partial u^*}{\partial n}(\mathbf{x}, \mathbf{x}_i) d\mathbf{x}. \tag{1.17}$$

Then, for a particular point $\mathbf{x}_i$ one can write

$$u_i + \sum_{j=1}^{N} \overline{H}_{ij} u_j = \sum_{j=1}^{N} G_{ij} q_j. \tag{1.18}$$

Let us now call

$$H_{ij} = \overline{H}_{ij} + \frac{1}{2}\delta_{ij},$$

where δ_{ij} is the Kronecker delta, in such a way that the $\frac{1}{2}$ value is summed to $\overline{H}$ when $i = j$. Then Equation (1.18) can now be written as

$$\sum_{j=1}^{N} H_{ij} u_j = \sum_{j=1}^{N} G_{ij} q_j. \tag{1.19}$$

If it is now assumed that the position of node $\mathbf{x}_i$ also varies from $i = 1$ to $i = N$, *i.e.* one assumes that the fundamental solution is applied at each node successively, defining a equation for each boundary node, a system of equations is obtained. This set of equations can be expressed in matrix form as

$$\mathbf{H}\mathbf{u} = \mathbf{G}\mathbf{q} \tag{1.20}$$

where $\mathbf{H}$ and $\mathbf{G}$ are two $N \times N$ matrices, and u and q are vectors of length N containing the boundary values of u and q at each boundary node.

Notice that N_1 values of u and N_2 values of q are unknown on Γ_1 and Γ_2 respectively ($N_1 + N_2 = N$), hence there are only N unknowns in the

system of equations (1.20). Once this boundary conditions are introduced into (1.20) one has to rearrange the system. Once all unknowns are passed to the left-hand side one can write

$$\mathbf{A}\mathbf{x} = \mathrm{b} \tag{1.21}$$

where $\mathbf{x}$ is a vector of unknown boundary values of u and q, and b is found by multiplying the corresponding columns of $\mathbf{H}$ or $\mathbf{G}$ by the known boundary values. It results interesting to point out that the unknowns are now a mixture of the potential and the normal derivative. This is a consequence of the boundary element method being a "mixed" formulation, and constitutes an important advantage over finite elements, Partridge [18]. Three cases may now be recognized, Pozrikidis [22]:

- If all element values u_j are specified, equation (1.19) provides us with a system of linear equations for the unknown vector of normal derivatives q.

- If all element values q_j are specified, equation (1.19) provides us with a system of inear equations for the unknown vector u.

- If some element values u_j, and a complementary set of values q_j are specified, equation (1.19) provides us with a system of linear equations for the unknowns, Equation (1.21).

Setting up the algebraic system (1.19) is the main task of the boundary element implementation. Once this has been accomplished, the solution can be found using a linear solver.

An important feature of the linear system arising from the boundary-element collocation method is that the coefficient matrices $\mathbf{H}$ and $\mathbf{G}$ are dense. In contrast, linear systems arising from finite-diference, finite-element, and spectral-element methods are banded.

Interior Solution

Once the element values u_j and q_j are available, we are be able to approximate the field value $u(\mathbf{x}_i)$ in terms of the influence coefficients. From (1.24) we state

$$u_i = \int_\Gamma q u_i^* d\Gamma - \int_\Gamma u q_i^* d\Gamma. \tag{1.22}$$

Note that the coefficient $\frac{1}{2}$ is taken as 1 and the fundamental solution is considered to be acting at an internal point. This process leads one to a direct integration of the influence coefficients. Considering the same discretization that was used for the boundary integrals at we obtain from (1.22)

$$u_i \simeq \sum_{j=1}^{N} G_{ij} q_j - \sum_{j=1}^{N} u_j \overline{H}_{ij} u_j. \tag{1.23}$$

Once the influence coefficients are calculated, Equation (1.23) describes a full solution in terms of the boundary values. Moreover, we are able to reproduce the boundary values using this discrete representation. Jaswon exploits this idea to bound the absolute error of the method for the Dirichlet problem [13].

Evaluation of integrals

The coefficients G_{ij} and $\overline{H}_{ij}$ can be calculated using a numerical integration formulae for the case $i \neq j$, Pozrikidis [22]. Lets assume first that the evaluation point $\mathbf{x}_i$ lies off the j-th boundary element, Figure 1.6. Using
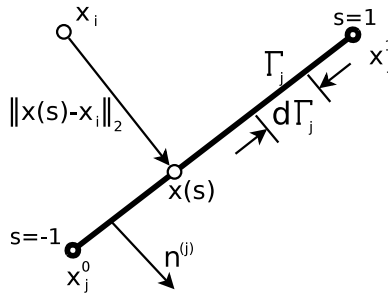

Figure 1.6: Non singular integral evaluation

parametrization (1.14) to describe the line elements, the differential arc length is given by

$$d\Gamma_j = \sqrt{x'(\xi)^2 + y'(\xi)^2} = h_\xi d\xi.$$

where $-1 \leq \xi \leq 1$, and

$$h_\xi \equiv \frac{1}{2} \sqrt{(x_j^0 - x_j^l)^2 + (y_j^0 - y_j^l)^2}.$$

is the metric coefficient associated with the parameter ξ. The unit normal vector to this element is constant and denoted by $n^{(j)}$, Figure 1.6. Accordingly, the influence coefficients are given by

$$G_{ij} = h_\xi \int_{-1}^{1} u^*(\mathbf{x}(\xi), \mathbf{x}_i)d\xi,$$

and

$$\overline{H}_{ij} = h_\xi \int_{-1}^{1} \left[\nabla q^*(\mathbf{x}(\xi), \mathbf{x}_i) \cdot \mathrm{n}^{(j)}\right] d\xi.$$

Developing the fundamental solution we get the integral-coefficients

$$G_j(\mathbf{x}_i) = -\frac{h_\xi}{2\pi} \int_{-1}^{1} \ln \|\mathbf{x}(\xi) - \mathbf{x}_i\|_2 d\xi,$$

and

$$H_j(\mathbf{x}_i) = -\frac{h_\xi}{2\pi} \int_{-1}^{1} \frac{\mathrm{n}^{(j)} \cdot (\mathbf{x}(\xi) - \mathbf{x}_i)}{\|\mathbf{x}(\xi) - \mathbf{x}_i\|_2^2} d\xi.$$

Here, the normal outward vector is given by the parametrization itself

$$n^{(j)} = [y'(\xi), -x'(\xi)].$$

In the case where $\mathbf{x}_i$ and $\mathbf{x}_j$ are on the same element, *i.e.* $i = j$, the solution requires a more accurate integration scheme, Figure 1.7, Pozrikidis [22]. In this case, as the integration point $\mathbf{x}$ approaches the evaluation point
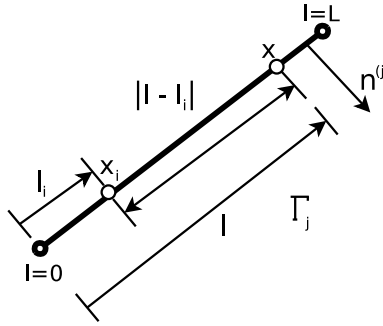

Figure 1.7: Singular integral evaluation

$\mathbf{x}_i$, the integrands of the influence coefficients (1.16) and (1.17) exhibit, respectively, a logarithmic and an apparent higher-order singularity, and the

boundary elements are classified as singular. Writting $\|\mathbf{x}_i - \mathbf{x}\|_2 = \|l_i - l\|$ and carrying out the integration of the point source distribution (1.16), we obtain

$$
\begin{aligned}
G_{ij} &= -\frac{1}{2\pi} \int_0^L \ln \|l - l_i\|_2 dl \\
&= -\frac{1}{2\pi} \left[l_i(\ln l_i - 1) + (L - l_i)(\ln (L - l_i) - 1) \right]
\end{aligned}
$$

where $L = \sqrt{(x_i^0 - x_i^l)^2 + (y_i^0 - y_i^l)^2}$. If we consider that the singular point x_i is halfway at the straight element E_j, then the previous equation becomes

$$
G_{ij} = -\frac{L}{2\pi}(\ln l_i - 1).
$$

Because the normal vector n is orthognonal to the tangential vector $(\mathbf{x} - \mathbf{x}_0)$, the numerator of the fraction inside the integral of the coefficient defined by (1.17) vanishes, and the influence coefficient is identically equal to zero, $H_{ij} = 0$.

1.3 First Order BEM

Up to this section only the case of constant elements, *i.e.* those with values of the variables assumed to be the same all over the element, has been discussed. Let us now consider a linear variation of u and q over each element, for which case the nodes are considered to be at the ends of each straight segment, Figure 1.5. This formulation is stated as 1-BEM, *i.e.* a first order boundary element method . Prior this point we have assumed that the boundary point x_i lies on a smooth boundary Γ, as we will see next, this is not always the be best assumption. First, lets discuss what happens when we drop the assumption of smoothness in the boundary.

Non-Smooth Boundaries

Suppose that x_i is defined over a corner of the boundary with internal angle $\gamma(x_i)$. Then we can evaluate (1.11) as

$$
\beta(x_i)u(x_i) + \int_\Gamma u(x, x_i)\frac{\partial u^*}{\partial n}(x)dx = \int_\Gamma u^*(x)\frac{\partial u}{\partial n}(x, x_i)dx, \qquad (1.24)
$$

where,

$$\beta(x_i) = \frac{\gamma(x_i)}{2\pi}.$$

This result is discussed by Brebbia [3], and follows by defining a small circular region around the point and then taking its radius to zero, similar to what has been shown in the process of deriving (1.11), Figure 1.8.
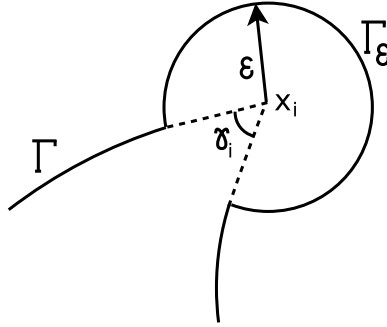

Figure 1.8: Extended boundary to evaluate (1.7) at a cusp boundary point

The general form of the integral representation is stated by defining $\beta(x_i)$ as a parameter takes the following values:

$$\beta(x_i) = \begin{cases} 1 & \text{if } x_i \in \Omega, \\ 0.5 & \text{if } x_i \in \Gamma \ \text{smooth}, \\ \dfrac{\gamma_i}{2\pi} & \text{if } x_i \in \Gamma \ \text{corner}. \end{cases}$$

Boundary Element Discretization

After discretizing the boundary into a series of N elements, equation (1.24) can be written as in the previous section:

$$\beta_i u_i + \sum_{j=1}^{N} \int_{\Gamma_j} u q_i^* d\Gamma_j = \sum_{j=1}^{N} \int_{\Gamma_j} q u_i^* d\Gamma_j \tag{1.25}$$

The integrals in this equation are more difficult to evaluate than those for the constant element as u and q vary linearly over each element Γ_j and hence it is not possible to take them out of the integrals.

Consider the *j-th* element. A linear variation of the interest values can be constructed in a similar way as we did with (1.14). The values of u and q at any point on the element can be defined in terms of their nodal values and the two linear interpolation functions ϕ^+ and ϕ^-, Figure 1.9,

$$\phi^+(\xi) = \tfrac{1}{2}(1 + \xi),$$

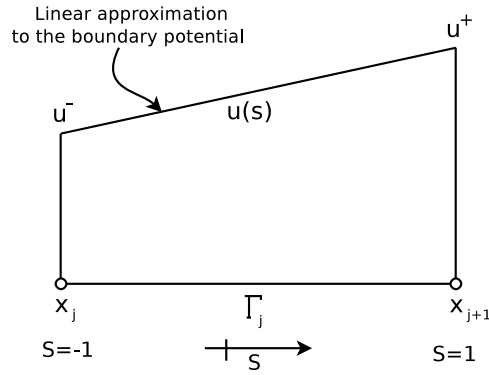$$\phi^-(\xi) = \tfrac{1}{2}(1 - \xi).$$

Following a linear parametrization

Figure 1.9: Linear variation at u over the boundary element

$$u(\xi) = \phi^- u^- + \phi^+ u^+ = [\phi^- \ \phi^+] \begin{bmatrix} u^- \\ u^+ \end{bmatrix},$$

$$\tag{1.26}$$

$$q(\xi) = \phi^- u^- + \phi^+ q^+ = [\phi^- \ \phi^+] \begin{bmatrix} q^- \\ q^+ \end{bmatrix},$$

where the dimensionless parameter ξ goes from -1 to 1 as the values of u or q varies from one node to another, and the extreme values are defined as

$$u^- := u_j^0, \quad u^+ := u_j^l,$$

$$q^- := q_j^0, \quad q^+ := q_j^l.$$

Then the integrals over an element j must be calculated. For the left-hand side of (1.25),

$$\int_{\Gamma_j} u q_i^* d\Gamma_j = \int_{\Gamma_j} q_i^* [\phi^- \ \phi^+] \begin{bmatrix} u^- \\ u^+ \end{bmatrix} = [h_{ij}^- \ h_{ij}^+] \begin{bmatrix} u^- \\ u^+ \end{bmatrix}, \tag{1.27}$$

where, for each element j, we have two terms

$$h_{ij}^+ = \int_{\Gamma_j} \phi^+ q_i^* d\Gamma_j$$

$$h_{ij}^- = \int_{\Gamma_j} \phi^- q_i^* d\Gamma_j.$$

Similarly, the integral on the right-hand side of (1.25) gives

$$\int_{\Gamma_j} q u_i^* d\Gamma_j = \int_{\Gamma_j} u_i^* \begin{bmatrix} \phi^- & \phi^+ \end{bmatrix} \begin{bmatrix} q^- \\ q^+ \end{bmatrix} = \begin{bmatrix} g_{ij}^- & g_{ij}^+ \end{bmatrix} \begin{bmatrix} u^- \\ u^+ \end{bmatrix}, \qquad (1.28)$$

where, for each element j, we have two terms

$$g_{ij}^+ = \int_{\Gamma_j} \phi^+ u_i^* d\Gamma_j$$

$$g_{ij}^- = \int_{\Gamma_j} \phi^- u_i^* d\Gamma_j.$$

Treatment of Corners

In general, a boundary element discretization will present a series of points of geometric discontinuity which require special attention. To study this particular case lets assume that we will discretize a boundary where each node is a cornered node. One option is to replace the cornered boundary by a smooth curve that resembles the cornered element. A less aggressive approach, taken from Partridge [18], is taken in this project and is discussed up next.

When the boundary of a region is discretized into linear elements, the final node of element j is the same point as the first node of element $j + 1$. Lets call flux at the normal derivative of u at a given point. While corners with different values of the flux on both sides exists in many practical problems, discontinuous values of the potential are seldom prescribed. Since the potential is unique at any point of the boundary, u^+ of element Γ_j and u^- of element Γ_{j+1} have the same value. However, this argument cannot be applied as a general rule to the flux, Figure 1.10.

To take into account the possibility that the flux at the final node of any element may be different from the flux at the initial node of the next element,
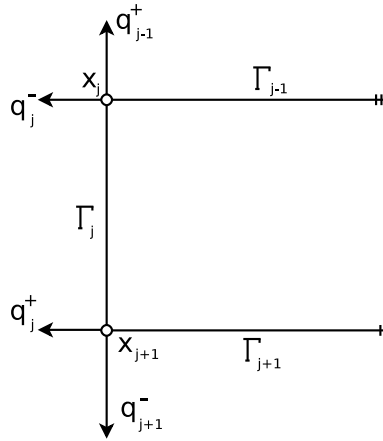
Figure 1.10: Flux discontinuity at boundary cusp

the fluxes can be arranged in a $2N$ vector, two flux values for each corner node, Figure 1.10,

$$\mathsf{q} = [q_0^-, \ q_0^+, \ldots, q_N^-, \ q_N^+]^T.$$

Substituting (1.27) and (1.28) at all the $j-$elements of (1.25) it follows, for node x_i,

$$\beta_i u_i + \sum_{j=1}^{N} \overline{H}_{ij} u_j = \sum_{j=1}^{N} [g_{ij}^- \ g_{ij}^+] \begin{bmatrix} q_j^- \\ q_j^+ \end{bmatrix}.$$

Here, the influence coefficients are defined as

$$\overline{H}_{ij} = h_{i,j-1}^- + h_{i,j}^+.$$

Evaluating at each boundary node we generate a system with N equations. Similarly as was previously shown for constant elements, (1.20), this whole set of equations can be written in matrix form

$$\mathbf{H}\mathsf{u} = \mathbf{G}\mathsf{q},$$

where $\mathbf{G}$ is a rectangular matrix of size $N \times 2N$, and q gives two values at each node to take into account possible flux discontinuities.

Several situations may occur at a boundary node. First, that the boundary is smooth at the node; in such a case, both fluxes "before" and "after" the node are the same unless they are prescribed different. In any case, only

one variable will be unknown, either the potential or the unique flux. Second, that the node is a corner point. In this case there are four possibilities depending on the boundary conditions:

1. Known values: fluxes "before" and "after" the corner.
   Unknown values: potential.

2. Known values: potential and flux "before" the corner.
   Unknown values: flux "after" the corner.

3. Known values: potential and flux "after" the corner.
   Unknown values: flux "before" the corner.

4. Known values: potential.

There is only one unknown per node for the first three cases. Then, the two known values are taken to the right-hand side and the usual system of $N \times N$ equations is obtained, as we did to generate (1.21).

When the number of unknowns at a corner node is two (case 4), one extra equation is needed for the node. The problem can also be solved using the idea of "discontinuous" elements [6]. In this case, the second node of element Γ_j and the first node of element Γ_{j+1} are shifted inside the two linear elements which meet at the corner and remain as two distinct nodes instead of joining into one at the corner, Figure 1.11. Thus, one equation can be written for each node. The potential and the flux are represented by linear functions along the whole of the element in terms of their nodal values, buy they are in principle discontinuous at the corner.

BEM Improvement

The uniform-element and linear discretizations described represent the simplest implementation of the Boundary Element Method. If a continuous boundary distribution for the function u, or its normal derivative q, is desired, then a higher-order discretization must be applied. Cubic splines and Lagrange polynomials are some examples that are discussed at [22].

The accuracy of a Boundary Element Method may be improved in two ways, Pozrikidis [22]: (a) by increasing the number of boundary elements while keeping the order of the polynomial expansion over each element constant, (This is an h-type refinement) or (b) by increasing the order of the
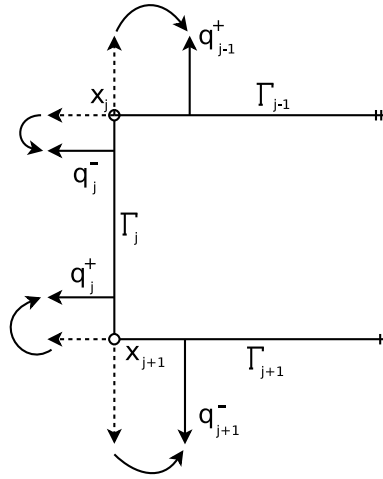
Figure 1.11: Flux shifting at at boundary cusp

polynomial expansion while keeeping the number of elements fixed (This is a *p*-type refinement).

   This work concentrates at the implementation of a first order BEM with straight line elements, which has been developed through the previous sections. Future work on the matter could include some refinement on the code to implement a more accurate version of the BEM.

1.4   Developed Examples

Laplace's Equation on a Square

Laplace's equation in two dimensions is given by

$$\frac{\partial^2 u}{\partial x^2} + \frac{\partial^2 u}{\partial y^2} = 0. \tag{1.29}$$

Let the unit square have a Dirichlet boundary condition $u = 0$ everywhere except $y = 1$, where the condition is $f(x)$ for $0 < x < 1$. The formal solution is

$$u(x, y) = \sum_{n=1}^{\infty} c_n \sinh(n\pi y) \sin(n\pi x), \tag{1.30}$$

where

$$c_n = 2 \int_0^1 f(x) \frac{\sin(n\pi x)}{\sinh(n\pi)} dx.$$

Solutions for boundary conditions on other sides of the square are obtained by switching variables in the formula, [23].

The solution of the problem was calculated using Wolfram Alpha CDF Player and the script constructed by David von Seggern [26]. The demomon-startion deals with the square $-0.5 < x < 0.5$ and $-0.5 < y < 0.5$ by shifting the variables, leading to a slightly more complicated solution.

To study the performance of the numerical method we define the following boundary condition:

$$\bar{u} = \begin{cases} 0, & x = 0.5, & -0.5 < y < 0.5 \\ 0, & x = -0.5, & -0.5 < y < 0.5 \\ 0, & y = 0.5, & -0.5 < x < 0.5 \\ f(x), & y = -0.5, & -0.5 < x < 0.5 \end{cases}$$
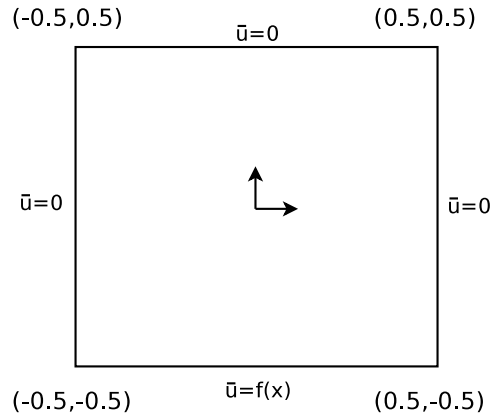
Figure 1.12: Boundary conditions for Laplace's problem

where the values for $y = -0.5$ are given by $f(x) = 1 - 4x^2$.

The solution (1.30) is approximated up to 4 terms and its graphic presented on Figure(1.13, Left). Then a second order boundary element method, *i.e.* using linear aproximations on the boundary elements, was developed to approximate the solution to the problem, Figure (1.13, Right).

A boundary discretization of 32 linear-boundary elements was defined to approximate the solution to Laplace's problem using the boundary element
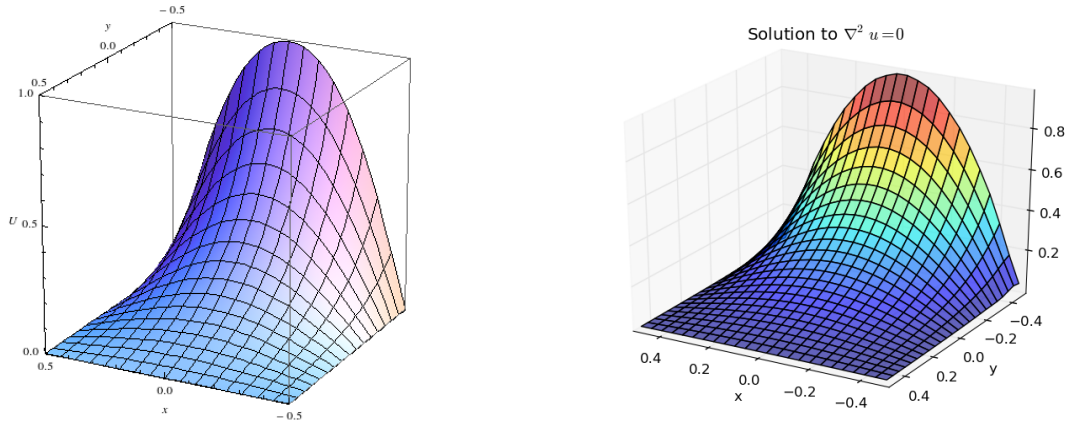
Figure 1.13: Solution to the Laplace's Equation: Approximated up to four terms (Left); Approximated using Boundary Element Method (Right)

method, Figure(1.14, Left). Once the boundary values are recovered using (1.24), the solution becomes available at any interior point, Equation (1.8). Then a square mesh of 64 interior points, Figure(1.14, Right), was defined and the solution at each point was calculated, Figure(1.13, Right). Lets remark that the high-density mesh is not strictly necessary for the solution to be calculated and it is defined only to set a smooth surface on Figure (1.13). Numerical values to compare the performance of the boundary element method will be discussed on following sections.

The next step is to compare the performance of the boundary element method using the two approximations discussed. At Figure 1.15 and Figure 1.15 we present the comparative BEM results using constant values over each boundary element and a linear variation over each. As we can see the constant value BEM presents solutions with less uniformity than first order BEM. Also, information in the corners of the problem is miss-treated when BEM-0 is applied. This variations on both methods depend mainly in the fact that BEM-1 is considering information at the corners of the boundary, while BEM-0 does not.
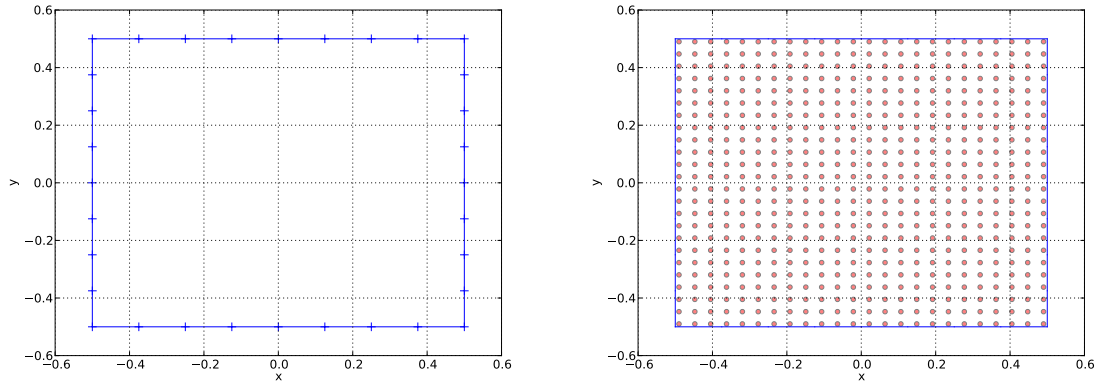
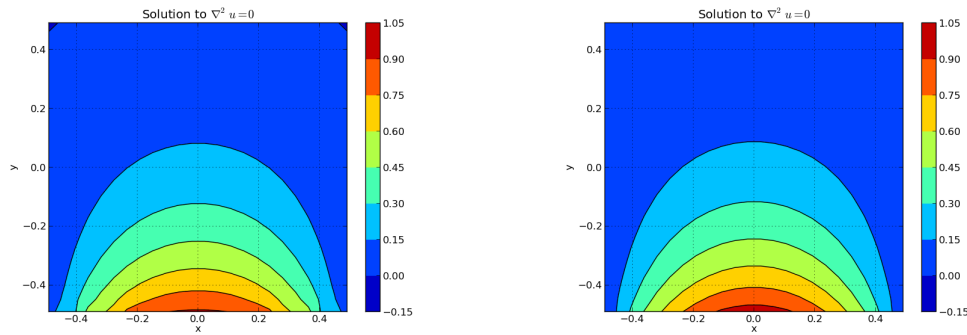Figure 1.14: Boundary discretization for BEM (Up), Interior nodes for BEM (Down)

Figure 1.15: BEM-Contour plots to Laplace's solution using: a constant value integration (Left), lineal variation integration (Right)

Laplace's equation on a smooth domain

We now solve Laplace's equation on a smooth domain, Figure 1.17. Here an ellipse of semi-major axis of length 2 and a semi-minor axis of length 1 is discretized using 16 linear boundary elements. Homgeneous boundary conditions cannot be prescribed for Laplace's equation as the result will be $u = q = 0$ at all nodes, Maximum principle. As a consequence, a non-homogeneous boundary condition has to be imposed. For this particular
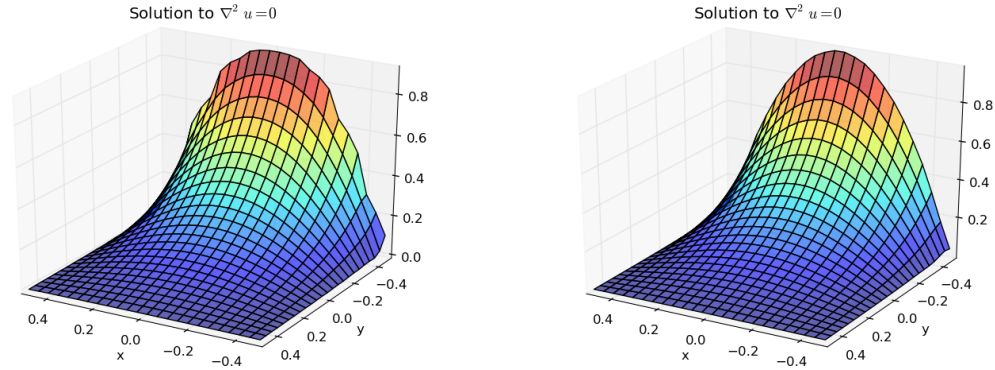
Figure 1.16: BEM-Surface plots to Laplace's solution using: a constant value integration (Left), lineal variation integration (Right)
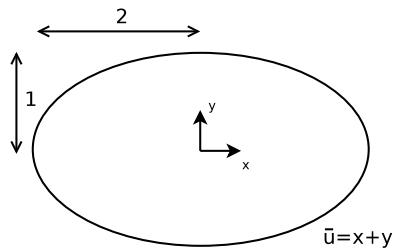

Figure 1.17: Elliptic smooth domain for Laplace's equation

problem lets set the boundary values of u as

$$\overline{u} = x + y.$$

It can be easily verified that $u = x + y$ is a particular solution to the problem.

The nodal boundary values are taken as the central points of each straight element for BEM-0 and the vertices for BEM-1, Figure 1.18. The solution is calculated at 17 interior points. The results are presented at Table 1.1.

In the coming chapters we will use BEM-0 to solve different problems on smooth boundaries. For domains with cusps, we take advantage of BEM-1 to solve the problem and recover information at the corners. BEM-1 will result essential to solve the problem of advective diffusive transport at chapter 3.
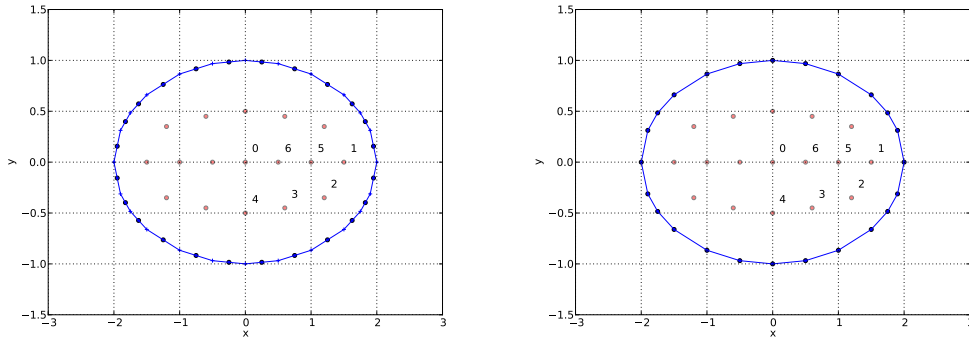
Figure 1.18: Smooth boundary discretization: nodal points for constant order BEM (Left), nodal points for first order BEM (Right)

Node	x	y	BEM-0	BEM-1	Solution
0	0	0	0	0	0
1	1.5	0	1.4936	1.5841	1.50
2	1.2	-0.35	0.8425	0.8904	0.85
3	0.6	-0.45	0.1504	0.1602	0.15
4	0	-1.5	-0.4985	-0.5110	-1.5
5	1.0	0	0.9956	1.0437	1.00
6	0.5	0	0.4985	0.5194	0.50

Table 1.1: Results for Laplace's equation on a elliptic domain using BEM

Chapter 2

BEM for Poisson's Equation

In previous chapter, we have discussed integral representations, integral equations, and boundary element methods for Laplace's equation. As we have seen, applying the Boundary Element Method to differential equations of the general form

$$L[u(x)] = 0,$$

is possible as long as the differential operator $L[\cdot]$ is linear, elliptic, homogeneous, and a fundamental solution for L is available. Asking for all this conditions to accomplish is no easy task. Commonly, we encounter models involving inhomogeneous, non-linear, and time-dependent (parabolic or hyperbolic) equations, expressing evolution from an initial state.

As we will see, the fundamental solution to the operator L has to take into account all the terms in the governing equation for the method to work, Partridge [18]. If this is not accomplished, domain integrals arise in the formulation of the boundary integral equation. The evaluation of domain integrals considerably increases the amount of data needed to apply the method and hence it losses some of its attractiveness in relation to Finite Element Method or other domain techniques.

To take advantage of the boundary-integral formulation, we must extend the theoretical foundation and numerical implementation of BEM, so that we can tackle a broader class of equations. In this chapter, we discuss the generalization of the boundary-integral formulation to have available a technique that: (i) Enables a "boundary-only" solution to be obtained for non-homogeneous problems, (ii) it can be easily extended to problems for which a fundamental solution is not available, (iii) can be applied using a similar approach for different problems.

2.1 Sources and Domain Integrals

Domain integrals in boundary elements may arise due to a variety of effects such as body forces, initial states, non-linear terms and other source terms. In what follows, the use of the non-homogeneous Poisson's differential equation will be studied to extend the BEM for non-homogeneous problems. The resulting formulation will later on be extended to cases for which the right-hand side term is, amongst others, a function of space, the potential itself or includes time-dependent effects.

Consider Poisson's equation,

$$\nabla^2 u = b, \quad \text{in } \Omega$$

where b is assumed to be a known function. Multiplying both sides by the fundamental solution of Laplace's equation u_i^*, and using Green's second identity one gets, Partridge [18],

$$\beta_i u_i + \int_\Gamma u q_i^* d\Gamma + \int_\Omega b u_i^* d\Omega = \int_\Gamma q u_i^* d\Gamma. \tag{2.1}$$

Which represents an integral equation for the function u evaluated at the point x_i.

Notice that although the b function is known, and consequently the integral in Ω do not introduce any new unknowns, the problem has changed in character; now we need to carry out a domain integral as well as the boundary integralss, Partridge [18]. The constant β_i as explained before, depends only on the boundary geometry at the point x_i under consideration. A simple way of solving (2.1) without having to compute any domain integrals is by changing the variables in such a manner that these integrals disappear. The fundamental part of this procedure consists in splitting the function into a homogeneous and a particular solutions, Partridge [18].
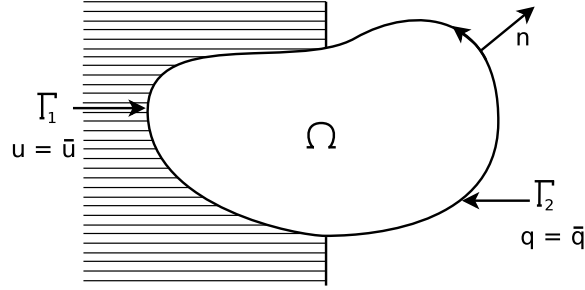
2.2 The Use of Particular Solutions

It results convenient to introduce the stated method with reference to Poisson's equation in two dimensions. Consider the boundary problem

$$\nabla^2 u = b, \quad \text{in } \Omega, \tag{2.2}$$

with the same boundary conditions as for Laplace's problem:

1. "Essential" conditions of the type $u = f$ on Γ_1.

2. "Natural" conditions such as $q := \dfrac{\partial u}{\partial n} = g$ on Γ_2.

Figure 2.1: Bidimensional domain Ω for Laplace's equation.

Assume now that the potential function u can be written as

$$u = \tilde{u} + \hat{u}, \qquad (2.3)$$

where $\tilde{u}$ is harmonic, and $\hat{u}$ is a particular solution such that

$$\nabla^2 \hat{u} = b.$$

Using Green's second identity, the domain integral in (2.1) becomes

$$
\begin{aligned}
\int_\Omega b u_i^* d\Omega &= \int_\Omega (\nabla^2 \hat{u}) u_i^* d\Omega \\
&= \int_\Omega \hat{u}(\nabla^2 u_i^*) d\Omega + \int_\Gamma u_i^* \hat{q} d\Gamma - \int_\Gamma q_i^* \hat{u} d\Gamma \\
&= \beta_i \hat{u}_i (\nabla^2 u_i^*) + \int_\Gamma u_i^* \hat{q} d\Gamma - \int_\Gamma q_i^* \hat{u} d\Gamma, \qquad (2.4)
\end{aligned}
$$

where $\hat{q} = \dfrac{\partial \hat{u}}{\partial n}$. Substituting (2.4) in (2.1),

$$\beta_i u_i + \int_\Gamma u q_i^* d\Gamma - \int_\Gamma q u_i^* d\Gamma = \beta_i \hat{u}_i + \int_\Gamma \hat{u} q_i^* d\Gamma - \int_\Gamma \hat{q} u_i^* d\Gamma. \qquad (2.5)$$

Notice that now all integrals are computed only along the boundary. Equation (2.5) can be written in a more compact form as a function of the new variable $\tilde{u} = u - \hat{u}$ as follows,

$$\beta_i \tilde{u}_i + \int_\Gamma \tilde{u} q_i^* d\Gamma = \int_\Gamma \tilde{q} u_i^* d\Gamma.$$

Formula (2.5) defines a boundary integral equation for the solution to the Poisson's equation at x_i, $u_i = u(x_i)$. It can be written, after a boundary discretization procedure, as

$$\beta_i u_i + \sum_{j=1}^{N} \overline{H}_{ij} u_j - \sum_{j=1}^{N} G_{ij} q_j = \beta_i \hat{u}_i + \sum_{j=1}^{N} \overline{H}_{ij} \hat{u}_j - \sum_{j=1}^{N} G_{ij} \hat{q}_j. \qquad (2.6)$$

Applying the above to all boundary points produce the following system

$$\mathbf{H}u - \mathbf{G}q = \mathbf{H}\hat{u} - \mathbf{G}\hat{q}, \qquad (2.7)$$

or simply,

$$\mathbf{H}u - \mathbf{G}q = d,$$

where,

$$d = \mathbf{H}\hat{u} - \mathbf{G}\hat{q}$$

is a vector that depends on the particular solution $\hat{u}$.

The main disadvantage of this approach is the need to describe the behaviour of the function $\hat{u}$ in an analytical form, which in some cases may be difficult or impossible to do. The next step is to generalize to account for arbitrary or unknown types of sources. This ideas gave origin to the Dual Reciprocity Method, first proposed by Nardini and Brebbia in 1983 [15].

2.3 The Dual Reciprocity Method

The DRM (Dual Reciprocity Method), discussed by Partridge at [18], is a variation of the Boundary Element Method that allows us to deal with the deduction of particular solutions $\hat{u}$ during developing the solution to non-homogeneous problems. For sake of simplicity we develop the DRM theoretical basis and applications using Poisson's equation. One departs from (2.2),

$$\nabla^2 u = b, \ \text{in } \Omega.$$

Let the solution be described as (2.3),

$$u = \hat{u} + \tilde{u},$$

where $\tilde{u}$ is harmonic, and

$$\nabla^2 \hat{u} = b.$$

It results difficult to find a solution $\hat{u}$ that satisfies the above, particularly in the case of non-linear or time-dependend problems. The Dual Reciprocity Method proposes the expansion of the particular solution into a sum of particular functions $\hat{u}_k$, sometimes called parental functions, instead of the single function $\hat{u}$.
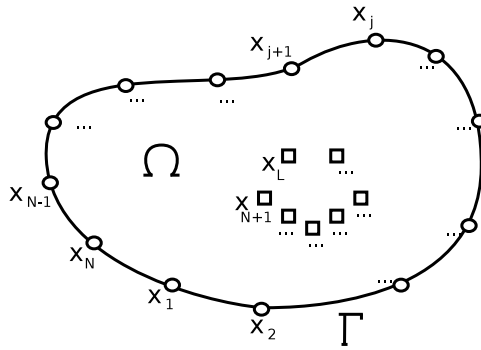

Figure 2.2: Interior and boundary nodes in the domain Ω.

We start the procedure by defining the nodal points: N in the problems boundary, and L inside the domain, Figure 2.2. Then we define a set of geometry-dependent functions f_k, $k = 1, \ldots, N + L$, such that

$$b \simeq \sum_{k}^{N+L} \alpha_k f_k. \tag{2.8}$$

Here, α_k correspond to a set of initially unknown coefficients, defined so that the equality is achieved at each nodal point. Each of the interpolating functions f_k, concisely called basis functions, maintain a close relation with each of the nodal points defined. Since equation (2.8) is defined to be exact at the nodal points, the expansion may be considered as valid over the whole problem's domain. At this moment, no restriction will be placed on the

functions f_k. Many different types may be used, each of which results in a different function $\hat{u}_k$. The question of which type of function f_k to use will be considered in the next section.

The particular solutions $\hat{u}_k$, and the approximating functions f_k are linked through the relation

$$\nabla^2 \hat{u}_k = f_k. \tag{2.9}$$

Substituting (2.9) at (2.8),

$$b = \sum_{k}^{N+L} \alpha_k(\nabla^2 \hat{u}_k).$$

Then, from Poisson's equation it follows

$$\nabla^2 u = \sum_{k}^{N+L} \alpha_k(\nabla^2 \hat{u}_k), \tag{2.10}$$

which demonstrates that the particular solution can be given, at the nodal points, by the expansion:

$$\hat{u} = \sum_{k}^{N+L} \alpha_k \hat{u}_k. \tag{2.11}$$

Up next we follow the same procedure as we did on the deduction of (2.1). Equation (2.10) is multiplied by the fundamental solution to Laplace's equation u_i^* then integrated over the whole domain Ω,

$$\int_\Omega (\nabla^2 u) u_i^* d\Omega = \sum_{k}^{N+L} \alpha_k \int_\Omega (\nabla^2 \hat{u}_k) u_i^* d\Omega. \tag{2.12}$$

Using Green's second identity at both sides of the last equation produces the following integral equation for the value of u at a source node $x_i \in \Omega$, [18],

$$\beta_i u_i + \int_\Gamma q_i^* u d\Gamma - \int_\Gamma u_i^* q d\Gamma =$$
$$\sum_{k=1}^{N+L} \alpha_k \left(\beta_i \hat{u}_{ik} + \int_\Gamma q_i^* \hat{u}_k d\Gamma - \int_\Gamma u_i^* \hat{q}_k d\Gamma \right). \tag{2.13}$$

The term $\hat{q}_k$ is defined as $\hat{q}_k = \frac{\partial \hat{u}_k}{\partial n}$. Also, we are establishing a nomenclature where the functions at the nodal point x_i are written as $\hat{u}_{ik} = \hat{u}_k(x_i)$, and $\hat{q}_{ik} = \hat{q}_k(x_i)$. The normal derivative $\hat{q}_k$ can be expanded as

$$\hat{q}_k = \frac{\partial \hat{u}_k}{\partial x} n_x + \frac{\partial \hat{u}_k}{\partial y} n_y, \qquad (2.14)$$

where n_x and n_y are the components of the outward normal to the boundary Γ. Note that equation (2.13) involves, again, no domain integrals. We got rid of the source term by first approximating b using (2.8), and then expressing both right and left sides of the resulting expression as boundary integrals using Green's second identity. The same result may be achieved using a reciprocity principle [15]. It is this operation which gives the name to the method: reciprocity has been applied to both sides of (2.12) to take all terms to the boundary, hence Dual Reciprocity Method.

The next step is to write (2.13) in discretized form. As a first approximation, we follow the same boundary discretization procedure as we did on section 1.2. Lets use the N boundary points as vertex to approximate the boundary using straight elements, Figure 2.3. Approximating the boundary
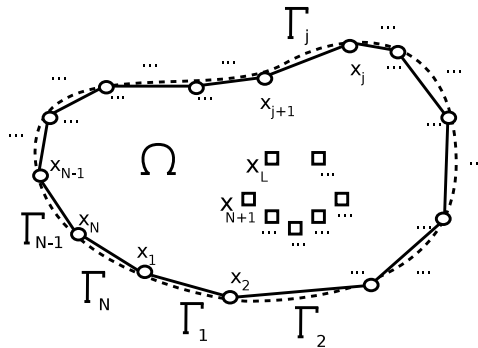

Figure 2.3: Boundary dicretization using straight elements for DRM.

by the union of the straight elements gives for a source node x_i the expresion

$$\beta_i u_i + \sum_{j=1}^{N} \int_{\Gamma_j} q_i^* u \, d\Gamma_j - \sum_{j=1}^{N} \int_{\Gamma_j} u_i^* q \, d\Gamma_j =$$
$$\sum_{k=1}^{N+L} \alpha_k \left(\beta_i \hat{u}_{ik} + \sum_{j=1}^{N} \int_{\Gamma_j} q_i^* \hat{u}_k \, d\Gamma_j - \sum_{j=1}^{N} \int_{\Gamma_j} u_i^* \hat{q}_k \, d\Gamma_j \right). \quad (2.15)$$

Now recast the center of each linear element as a nodal point x_j. Lets suppose that the functions u, q, $\hat{u}_k$ and $\hat{q}_k$ take constant values over each element, *i.e.*

$$u|_{\Gamma_j} = u_j, \qquad q|_{\Gamma_j} = q_j,$$

$$\hat{u}_k|_{\Gamma_j} = \hat{u}_{jk}, \quad \hat{q}_k|_{\Gamma_j} = \hat{q}_{jk},$$

then one can take out the constants from the integrals and write,

$$\beta_i u_i + \sum_{j=1}^{N} H_{ij} u_j - \sum_{j=1}^{N} G_{ij} q_j =$$
$$\sum_{k=1}^{N+L} \alpha_k \left(\beta_i \hat{u}_{ik} + \sum_{j=1}^{N} H_{ij} \hat{u}_{jk} - \sum_{j=1}^{N} G_{ij} \hat{q}_{jk} \right). \quad (2.16)$$

The influence coefficients are defined as in (1.16) and (1.17). This process could be easily extended to consider linear increments in each boundary element instead of constant values. The procedure is not presented, it follows the same steps as the one deducted at section 1.3, however results are discussed for non-smooth boundaries.

It may be noted that, since $\hat{u}_k$ and $\hat{q}_k$ are known functions once f_k is defined, there is no need to approximate their variation within each boundary element by using interpolation functions or constant nodal valuess, Partridge [18]. However, to do so implies that the same matrices **H** and **G** defined in Chapter 1 may be used on both sides of the equation. This procedure introduces an approximation in the evaluation of the terms on the right-hand side of equation (2.15), nevertheless, the error has been show to be small and the efficiency of the method to be considerably increased, Nardini [15].

After application to all boundary nodes using a collocation technique, and incorporating the terms involving β_i in the main diagonal of $\mathbf{H}$, equation (2.16) can be expressed in a matrix form as

$$\mathbf{H}u - \mathbf{G}q = \sum_{k=1}^{N+L} \alpha_j (\mathbf{H}\tilde{u}_k - \mathbf{G}\tilde{q}_k). \qquad (2.17)$$

If each of the vectors $\tilde{u}_k$ and $\tilde{q}_k$ is considered to be one column of the matrices $\tilde{\mathbf{U}}$ and $\tilde{\mathbf{Q}}$ respectively, then equation (2.17) may be written without summation to produce

$$\mathbf{H}u - \mathbf{G}q = (\mathbf{H}\tilde{\mathbf{U}} - \mathbf{G}\tilde{\mathbf{Q}})\alpha. \qquad (2.18)$$

Equation (2.18) is the basis for the application of Dual Reciprocity Boundary Element Method and involves discretization of the boundary only. Internal nodes may be defined in the number and at the locations desired by the user; this is generally done at points where it is desirable to know the interior solution.

The process described forms the basis of the dual reciprocity boundary element method (DRBEM). It establishes a procedure for extending the Boundary Element Method for solving non-linear, or time dependent problems. Two main issues must be distinguished, the case when the source term s depends only on the spatial coordinates, and the case when the source term s depends on the, *a-priori* unknown, function u.

Interior Nodes

The definition of interior nodes is not normally a necessary condition to obtain a boundary solution; however, the solution will usually be more accurate if a number of such nodes is used. When interior nodes are defined, each one is independently placed, and they do not form part of any element or cell, thus only the coordinates are needed as input data. Hence, these nodes may be defined in any order.

The α vector

The α vector in equation (2.18) will now be discussed. It was seen in equation (2.8) that

$$b_j = \sum_{k=1}^{N+L} \alpha_k f_{jk},$$

at each nodal point x_j. This defines a linear system that may be represented in matrix form as

$$b = \mathbf{F}\alpha, \tag{2.19}$$

where each column of $\mathbf{F}$ consists of a vector $\mathbf{f}_j$ containing the values of the function f_j at each of the DRM collocation points. Up to this point we have considered that the source term $b = b(x, y)$ as a known function. Thus, assuming that $\mathbf{F}$ may be inverted, we solve for α

$$\alpha = \mathbf{F}^{-1}b.$$

The right-hand side of equation (2.18) is thus a known vector

$$d = (\mathbf{H}\tilde{\mathbf{U}} - \mathbf{G}\tilde{\mathbf{Q}})\alpha.$$

Then (2.18) can be rewritten as

$$\mathbf{H}u - \mathbf{G}q = d. \tag{2.20}$$

Applying boundary conditions to (2.20), as explained in chapter 1, this equation reduces to the form

$$\mathbf{A}x = y,$$

where x contains N unknown boundary values of u or q. A full discussion of the implementation of different boundary conditions in BEM analysis can be found in [2].

Interior Solution

After solution of (2.20) for the unknown boundary values, the solution at any internal node can be calculated from equation (2.16). In the case of internal nodes, as was explained in chapter 1, $\beta_i = 1$ and (2.16) becomes

$$u_i = -\sum_{j=1}^{N} H_{ij}u_j + \sum_{j=1}^{N} G_{ij}q_j +$$

$$+ \sum_{k=1}^{N+L} \alpha_k \left(\beta_i \hat{u}_{ik} + \sum_{j=1}^{N} H_{ij}\hat{u}_{jk} - \sum_{j=1}^{N} G_{ij}\hat{q}_{jk} \right). \tag{2.21}$$

The development of DRM for Poisson-type equiations is now complete. In the next section, the different approximating functions f and the respective expressions for $\hat{u}$ and $\hat{q}$ will be considered.

2.4 f Expansions

The particular solution $\hat{u}$, its normal derivative $\hat{q}$, and the corresponding approximating functions f used in DRM analysis are not limited by the formulation except that the resulting $\mathbf{F}$, equation (2.19), should be non-singular. In order to define this functions it is customary to propose an expansion for f and then compute $\hat{u}$ and $\hat{q}$ using equations (2.9) and (2.14), respectively.

The DRBEM works by approximating source terms by a finite series of basis functions, usually radial basis functions, Golberg [10], in the form

$$f_k = 1 + r_k + r_k^2 + \ldots + r_k^m, \tag{2.22}$$

for which corresponds the functions $\hat{u}_k$ and $\hat{q}_k$:

$$\hat{u}_k = \frac{r_k^2}{4} + \frac{r_k^3}{9} + \ldots + \frac{r_k^{m+2}}{(m+2)^2}, \tag{2.23}$$

$$\hat{q}_k = \left(\frac{1}{2} + \frac{r}{3} + \ldots + \frac{r^m}{(m+2)} \right) \begin{pmatrix} x - x_k \\ y - y_k \end{pmatrix} \cdot n \tag{2.24}$$

where r_k is the euclidean distance

$$r_k(\mathbf{x}) = \|\mathbf{x} - \mathbf{x}_k\|_2, \quad \mathbf{x} \in \mathbb{R}^2$$

and n corresponds to the outer normal to the problem's boundary Γ. The expansion using some type of distance functions was adopted, first, by Nardini and Brebbia, then by most researchers, as the simplest and most accurate alternative [18]. However, Goldberg and Chen [9] suggested that thin plate splines might be a better and more mathematically defensible choice for bi-dimensional problems, [11].

$$f_k = r_k^2 \log r_k, \tag{2.25}$$

for which corresponds,

$$\hat{u}_k = \frac{1}{32} r_k^4 (\log r_k^2 - 1), \tag{2.26}$$

$$\hat{q}_k = \left(\frac{1}{4} r_k^2 \log r - \frac{1}{16} r_k^2, \right) (r_k \cdot n). \tag{2.27}$$

For the Dirichlet problem using Poisson's equation over a bounded domain in the plane, Golberg has showed that the error using DRM has to components, [9]: (1) that due to approximating the particular solution (which generally depends on the error in approximating the source term), and (2) error due to the choioce of boundary element method [11]. Using this as an argument it could be said that traditional BEMs using low order piecewise polynomial approximations that the dominant part of the computational error may be due to BEM error -not the interpolation error-; while if higher order solvers are used the dominant error may now be the interpolation error and the effects on the choice of radial basis functions is evident.

It is important to note that the matrix $\mathbf{F}$ depends only on geometric data and has no relation to either governing equation nor boundary conditions. It may be calculated once and stored in a data file for use with all subsequent analyses involving the same discretization.

For the method constructed in this thesis, the implementation of the DRBEM is based in two interpolating functions:

- $f_k(x) = 1 + r_k(x)$,

- $f_k(x) = r_k^2(x) \log r_k(x)$.

Several examples based on this interpolating functions are considered in the next sections. In all cases, results using thin plate approximating functions are found to differ little from those obtained using $1 + r_k$, which is the simplest alternative.

2.5 Developed Examples

We will start this section by considering a known source term $b = b(x, y)$. Then we will increase the complexity of the problem by introducing the potential u, the derivative u_x and a time dependent term u_t, and solve using DRBEM.

Examples here discussed are presented by Partridge at [18], we will be presented using two classes of source term approximations: a first order radial basis function and thin plate splines, and extend the results presented at [18] by considering two class of approximating functions. Results are defined over two domains: an elliptical domain of semi-axes with length 2 and 1, Figure 2.4 (Left); And a square domain of side-length 3, Figure 2.4 (Right).
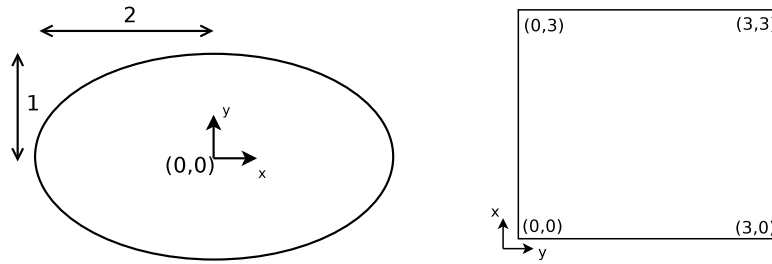
Figure 2.4: Smooth boundary (Left), Non-smooth boundary (Right).

The smooth domain is discretized using 24 linear boundary elements, and 17 interior nodes, Figure 2.5 (Left). The square domain is discretized by using 24 straight elements in the boundary and 33 interior nodes, Figure 2.5 (Right).
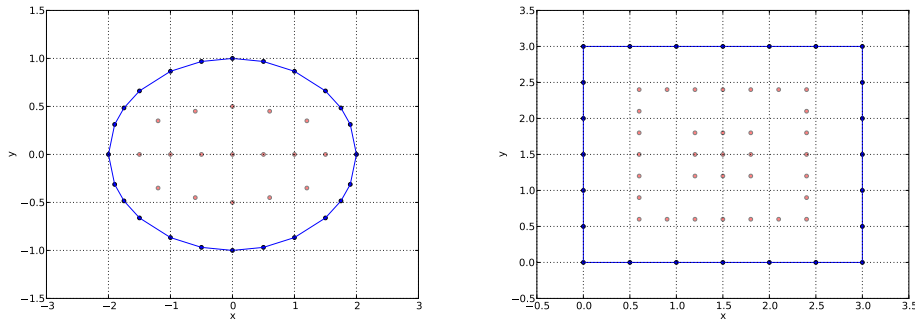

Figure 2.5: Smooth discrete boundary (Left), Non-smooth discrete boundary (Right).

2.5.1   The DRBEM for $\nabla^2 u = b(x, y)$

Since the method for solving this equation has already been discussed, in this section we only present results of the application of equation (2.18) to solve Poisson's problem.

The Case $\nabla^2 u = -x$

The governing equation is

$$\nabla^2 u = -x.$$

The problem's domain is defined over the smooth boundary Figure 2.4 (Left). For this case we consider an homogeneous boundary condition $u|_\Gamma = 0$. The exact solution is given by

$$u = \frac{2x}{7}\left(\frac{x^2}{4} + y^2 - 1\right),$$

and the flux is evaluated as

$$q = -\frac{x}{14}\left(\frac{3x^2}{2} + 2y^2\right) - \frac{4xy^2}{7}.$$

Zero order DRBEM, 0-BEM, gives the results presented in Table 2.1.

x	y	Exact	$f = 1 + r$	$f = r^2 \log r$
0	0	0	0	0
1.5	0	0.1875	0.1616	0.1784
1.2	-0.35	0.1774	0.1514	0.1673
0.6	-0.45	0.1213	0.1161	0.1189
0	-0.5	0	0	0
1	0	0.2143	0.1974	0.2057
0.5	0	0.1339	0.1279	0.1309

Table 2.1: Interior Values for 0-BEM to equation $\nabla^2 u = -x$

The Case $\nabla^2 u = a^2 - x^2$

The governing equation is

$$\nabla^2 u = 4 - x^2.$$

The problem's domain is defined over the smooth boundary Figure 2.4 (Left). For this case we consider an homogeneous boundary condition $u|_\Gamma = 0$. .The exact solution is given by

$$u = \left[1.6 - \frac{1}{246}\left(50x^2 - 8y^2 + 33.6\right)\right]\left(\frac{x^2}{4} + y^2 - 1\right),$$

and the flux is evaluated as

$$q = 0.4(x^2 + 8y^2) + \frac{1}{246}\left(-50x^3 - 96xy^2 + 83.2x\right)\frac{x}{2}$$
$$+ \frac{1}{246}\left(-96x^2y + 32y^3 - 83.2y\right)y.$$

Zero order BEM (considering constant values over each element), gives the results presented in Table 2.2.

x	y	Exact	$f = 1 + r$	$f = r^2 \log r$
0	0	-1.4634	-1.4475	-1.4505
1.5	0	-0.4402	-0.3963	-0.3704
1.2	-0.35	-0.6079	-0.5635	-0.5514
0.6	-0.45	-0.9883	-0.9713	-0.9556
0	-0.5	-1.1037	-1.0920	-1.0762
1	0	-0.9451	-0.9118	-0.9267
0.5	0	-1.3243	-1.3044	-1.3084

Table 2.2: Interior Values for 0-BEM to equation $\nabla^2 u = 4 - x^2$

2.5.2 The DRBEM for $\nabla^2 u = b(x, y, u)$

In this section, the range of application of the DRM will be extended to bi-dimensional problems governed by equations of the type

$$\nabla^2 u = b(x, y, u) \tag{2.28}$$

where the non-homogeneous term may be a combination, sum or product of functions. The source term could include linear as well as non-linear terms. In DRM analysis only truly non-linear problems are solved using iterative techniques. In this thesis we restrict our work to the case of linear non-homogeneous sources. In order to generate the basic relationships the case

$$\nabla^2 u + u = 0$$

is considered. Function b is defined as $-u$. Thus, from (2.19)

$$\alpha = -\mathbf{F}^{-1}\mathbf{u}.$$

For this class of problems it is no longer possible to separate boundary and interior solutions as the presence of the fully populated matrix $\mathbf{F}^{-1}$ results in a coupled problem in which both sets of values, interior and boundary ones, must be calculated simultaneously. The next step is to extend our linear system. Evaluating (2.16) at every node and substituting the vector α as the product $\mathbf{F}^{-1}$u then (2.18) becomes

$$\mathbf{H}u - \mathbf{G}q = -(\mathbf{H}\tilde{\mathbf{U}} - \mathbf{G}\tilde{\mathbf{Q}})\mathbf{F}^{-1}u. \tag{2.29}$$

The matrices $\mathbf{G}$, $\mathbf{H}$, $\tilde{\mathbf{Q}}$ and $\tilde{\mathbf{U}}$ of equation (2.29) are defined as the same as used in the previous sections, except that we extend them to include the interior nodes. The matrix $\mathbf{F}$ was defined in connection only with the calculation of vector α. Then dealing with problems governed by equation of the type (2.28), or the time-dependent cases to be discussed on the next section, α cannot be obtained explicitly and will always be expressed in the matrix equation as $\mathbf{F}^{-1}$b. The right hand of (2.29) thus becomes a matrix expression multiplying the unknown vector b which will be different in each case.

For the examples to be considered in this and the following sections, the right-hand side of (2.28) is an unknown function where the known vector d, equation (2.20), has to be replaced by a matrix expression, equation (2.29). Defining

$$\mathbf{S} = (\mathbf{H}\tilde{\mathbf{U}} - \mathbf{G}\tilde{\mathbf{Q}})\mathbf{F}^{-1} \tag{2.30}$$

then equation (2.20) becomes

$$\mathbf{H}u - \mathbf{G}q = -\mathbf{S}u. \tag{2.31}$$

The calculation of $\mathbf{S}$ is done by multiplying known matrices. Collecting terms in u on the left-hand produces

$$(\mathbf{H} + \mathbf{S})u = \mathbf{G}q. \tag{2.32}$$

Over the boundary, N values of u and q are unknown, while L values of u at interior nodes are all unknown. After applying the boundary conditions the usual equation

$$\mathbf{A}x = y$$

is obtained. This represents a $(N+L) \times (N+L)$ linear system and $\mathbf{x}$ contains N boundary values of u or q, plus L interior values of u.

Equations (2.29) to (2.32) form the basis of application of the Dual Reciprocity Method to equations of the type (2.28). The only difference in each new case will be a new vector b to replace $-u$. The treatment of these vectors will be explained for each case to be studied in a systematic way.

The Case $\nabla^2 u = -u$

The governing equation is

$$\nabla^2 u + u = 0.$$

We define the problem over the smooth boundary Figure 2.4 (Left). Since homogeneous boundary conditions will result in the trivial solution $u = q = 0$ at all nodes, a non-homogeneous condition has to be used, for instance

$$u = \sin x.$$

This equation results in a solution to the problem considered. Zero DRBEM, 0-BEM, gives the results presented on Table 2.3.

x	y	Exact	$f = 1 + r$	$f = r^2 \log r$
0	0	0	-0.0001	-0.0001
1.5	0	0.9975	0.9845	0.9981
1.2	-0.35	0.9320	0.9178	0.9173
0.6	-0.45	0.5646	0.5606	0.5596
0	-0.5	0	-0.0001	-0.0001
1	0	0.8415	0.8310	0.8332
0.5	0	0.4794	0.4748	0.4759

Table 2.3: Interior Values for 0-BEM to equation $\nabla^2 u + u = 0$

2.5.3 The DRBEM for $\nabla^2 u = b(x, y, u_x, u_y)$

In this section, the range of application of the DRM will be extended to bi-dimensional problems governed by equations of the type

$$\nabla^2 u = b(x, y, u_x, u_y) \tag{2.33}$$

where the non-homogeneous term may also be a combination, sum or product of functions. The term u_x and u_y represent the spatial derivatives of the

function u. Convective terms can be easily accommodated in the DRM treatment. Consider, as an example, an equation of the type

$$\nabla^2 u = \frac{\partial u}{\partial x}.$$

Comparing this with (2.28) it is seen that in this case $b = \frac{\partial u}{\partial x}$, such that the vector

$$\mathrm{b} = \frac{\partial \mathrm{u}}{\partial x}$$

represents the nodal values of the derivative of u with respect to x. Thus, substituting into equation (2.19), one obtains

$$\alpha = \mathbf{F}^{-1} \frac{\partial \mathrm{u}}{\partial x},$$

and equation (2.20) becomes for this case

$$\mathbf{H}\mathrm{u} - \mathbf{G}\mathrm{q} = (\mathbf{H}\tilde{\mathbf{U}} - \mathbf{G}\tilde{\mathbf{Q}})\mathbf{F}^{-1} \frac{\partial \mathrm{u}}{\partial x}, \tag{2.34}$$

or, using (2.30),

$$\mathbf{H}\mathrm{u} - \mathbf{G}\mathrm{q} = \mathbf{S} \frac{\partial \mathrm{u}}{\partial x}. \tag{2.35}$$

A mechanism must now be established to relate the nodal values of u to the nodal values of its derivative $\frac{\partial u}{\partial x}$. At this point it should be remembered that the basic appoximation of the DRM technique is equation 2.19,

$$\mathrm{b} = \mathbf{F}\alpha.$$

A similar equation may be written for u,

$$\mathrm{u} = \mathbf{F}\gamma, \tag{2.36}$$

where $\gamma \neq \alpha$. Differentiating (2.36) produces

$$\frac{\partial \mathrm{u}}{\partial x} = \frac{\partial \mathbf{F}}{\partial x}\gamma, \tag{2.37}$$

where, in the right hand side of the equation we find a $(N + L) \times (N + L)$ matrix which contains the derivatives of each of the approximating functions evaluated at each nodal point, *i.e.*

$$\left(\frac{\partial \mathbf{F}}{\partial x}\right)_{ij} = \frac{\partial f_j}{\partial x}(x_i).$$

Recasting (2.36) as $\gamma = \mathbf{F}^{-1}\mathrm{u}$ one can write (2.37) as

$$\frac{\partial \mathrm{u}}{\partial x} = \frac{\partial \mathbf{F}}{\partial x}\mathbf{F}^{-1}\mathrm{u}. \tag{2.38}$$

Substituting into (2.35) one obtains

$$\mathbf{H}\mathrm{u} - \mathbf{G}\mathrm{q} = \mathbf{S}\frac{\partial \mathrm{u}}{\partial x} = \mathbf{S}\frac{\partial \mathbf{F}}{\partial x}\mathbf{F}^{-1}\mathrm{u}. \tag{2.39}$$

Calling

$$\mathbf{R} = \mathbf{S}\frac{\partial \mathbf{F}}{\partial x}\mathbf{F}^{-1}, \tag{2.40}$$

produces the system of equations

$$(\mathbf{H} - \mathbf{R})\mathrm{u} = \mathbf{G}\mathrm{q}, \tag{2.41}$$

which can be handled exactly as (2.32).

Both $\frac{\partial \mathbf{F}}{\partial x}$ and $\mathbf{F}^{-1}$ are fully populated matrices. The terms in the $\frac{\partial \mathbf{F}}{\partial x}$ matrix depend on the basis-function used. For the radial-basis-functions (2.22) we have

$$\frac{\partial f}{\partial x} = (x - x_k)\left(\frac{1}{r} + 2 + 3r + \ldots + mr^{m-2}\right). \tag{2.42}$$

For the thin-plate-spline-functions (2.25) we have

$$\frac{\partial f}{\partial x} = (x - x_k)2\log(r + 1). \tag{2.43}$$

Is important to note that if we define the expansion (2.37) using the radial basis functions we will generate singularities at the source elements. This will cause problems with the diagonal elements of the matrix $\frac{\partial \mathbf{F}}{\partial x}$. To solve this problem we define the expansion in (2.37) as

$$\left.\frac{\partial u}{\partial x}\right|_{x_i} = \sum_{\substack{j=1 \\ j \neq i}}^{N+L} \gamma_j \left.\frac{f_j}{\partial x}\right|_{x_i}.$$

This solution is presented by Partridge at [18], and defines the matrix $\frac{\partial \mathbf{F}}{\partial x}$ as a skew-symmetric matrix. If we expand using thin plate spline functions not such problem arises and (2.37) is defined using the standard expansion

$$\left.\frac{\partial u}{\partial x}\right|_{x_i} = \sum_{j=1}^{N+L} \gamma_j \left.\frac{f_j}{\partial x}\right|_{x_i}.$$

A similar treatment can be carried out in the case of the equation

$$\nabla^2 u = \frac{\partial u}{\partial y}.$$

For which the same equation (2.29) will be obtained with

$$\mathbf{R} = \mathbf{S}\frac{\partial \mathbf{F}}{\partial y}\mathbf{F}^{-1}.$$

The derivatives are defined similarly as on (2.42) and (2.43), except that they are taken with respect to the space variable y.

The Case $\nabla^2 u = -\dfrac{\partial u}{\partial x}$

The governing equation is

$$\nabla^2 u + \frac{\partial u}{\partial x} = 0.$$

We define the problem over the smooth boundary Figure 2.4 (Left). A particular solution for this case is

$$u = e^{-x}$$

which, when imposed as an essential boundary condition, also constitutes the problem's solution. Zero order DRBEM 0-BEM, gives the results presented on Table 2.4.

2.5.4 The DRBEM for $\nabla^2 u = b(x, y, u_x, u_y, t)$

This section presents applications of the boundary element Dual Reciprocity Method to transient problems. For the DRM formulation, the fundamental solution of Laplace's equation is used and we consider problems in the general form

$$\nabla^2 u = b(x, y, u, t) \tag{2.44}$$

where the non-homogeneous term may also be a combination, sum or product of functions. We start by defining the method of solution for a diffusion

x	y	Exact	$f = 1 + r$	$f = r^2 \log r$
0	0	1.0000	1.0220	1.0306
1.5	0	0.2231	0.2211	0.2379
1.2	-0.35	0.3012	0.3312	0.3348
0.6	-0.45	0.5488	0.6315	0.6285
0	-0.5	1.0000	1.1576	1.1573
1	0	0.3679	0.3707	0.3829
0.5	0	0.6065	0.6199	0.6255

Table 2.4: Interior Values for 0-BEM to equation $\nabla^2 u + \dfrac{\partial u}{\partial x} = 0$

problem in this section. Then, in chapter 3, we will extend to the advective-diffusive transport equation. To state the basic relationships on the method we start with the bi-dimensional heat equation

$$\nabla^2 u = \frac{1}{k}\dot{u}.$$

The temporal derivative is taken using Newton notation as $\dot{u}$. The parameter k is a positive constant that refers to the thermal diffusivity. The definition of the problem is completed with the specification of appropriate boundary condition, and initial conditions $u(x, y, t_0) = u_0(x, y)$ at the problems domain. Comparing the heat equation with (2.28) it is seen that in this case $b = \frac{1}{k}\dot{u}$. The application of the DRM follows the same pattern as in previous sections, and produces a matrix equation of the form

$$\mathbf{H}u - \mathbf{G}q = \frac{1}{k}(\mathbf{H}\tilde{\mathbf{U}} - \mathbf{G}\tilde{\mathbf{Q}})\alpha \qquad (2.45)$$

In the present case, nevertheless, approximation (2.8) implies a separation of variables in which f_k are known geometry-dependen functions and α_k unknown functions of time,

$$\dot{u} = \sum_{k=1}^{N+L} f_k(x, y)\alpha_k(t). \qquad (2.46)$$

Thus, matrices $\tilde{\mathbf{U}}$ and $\tilde{\mathbf{Q}}$ above are the same as in the previous analysis. This can be represented as a linear system

$$\dot{\mathbf{u}} = \mathbf{F}\alpha \qquad (2.47)$$

The next step in the formulation similar to the inversion of equation (2.36), written in this case as

$$\alpha = \mathbf{F}^{-1}\dot{u}.$$

Substituting the vector α at (2.34) produces

$$\mathbf{H}u - \mathbf{G}q = \frac{1}{k}(\mathbf{H}\tilde{\mathbf{U}} - \mathbf{G}\tilde{\mathbf{Q}})\mathbf{F}^{-1}\dot{u}. \tag{2.48}$$

The term multiplying $\dot{u}$ can be seen as a "heat capacity" matrix,

$$\mathbf{C} = -\frac{1}{k}\mathbf{S} = -\frac{1}{k}(\mathbf{H}\tilde{\mathbf{U}} - \mathbf{G}\tilde{\mathbf{Q}})\mathbf{F}^{-1}.$$

And equation (2.31) is rewritten as

$$\mathbf{C}\dot{u} + \mathbf{H}u = \mathbf{G}q \tag{2.49}$$

To solve (2.49) a two-level time integration scheme is employed, [28]. A linear approximation is proposed for the variation of u and q within each time step, this leads to

$$u = (1 - \theta_u)u^m + \theta_u u^{m+1}, \tag{2.50}$$

$$q = (1 - \theta_q)q^m + \theta_q q^{m+1}, \tag{2.51}$$

$$\dot{u} = \frac{1}{\Delta t}(u^{m+1} - u^m), \tag{2.52}$$

where θ_u and θ_q are parameters that take values between 0 and 1, which position the values of u and q, respectively, between time levels m and $m+1$; and u^m and q^m represent the values of u and q at the time step m. Substituting these approximations into (2.49) yields:

$$\left(\frac{1}{\Delta t}\mathbf{C} + \theta_u\mathbf{H}\right)u^{m+1} - \theta_q\mathbf{G}q^{m+1} =$$

$$\left(\frac{1}{\Delta t}\mathbf{C} + (1 - \theta_u)\mathbf{H}\right)u^m - (1 - \theta_q)\mathbf{G}q^m \quad (2.53)$$

The right hand side of (2.53) is known at all times since it involves values which have been specified as initial conditions or calculated previously. Upon introducing the boundary conditions at time $(m + 1)\Delta t$, one can rearrange

the left side of (2.53) and solve the resulting system of equations for each time level.

Note that the elements of matrices **H**, **G**, and **S** depend only on geometrical data. Thus, they can all be computed once and stored. If the value of Δt is kept constant, the system matrix can be reduced only once as well, and the time advance procedure will consist of a simple recursive scheme with only algebraic operations involved.

The Case $\nabla^2 u = \dot{u}$

The problem of heat diffusion in a square plate, Figure 2.4 (Right), initially at $30°$ and cooled by the application of a thermal shock ($u = 0°$ all over the boundary) has been studied using the finite element method at [5]. The exact solution for this problem is given in the last reference as

$$u = \sum_{n=1}^{\infty} \sum_{j=1}^{\infty} A_{nj} \sin \frac{n\pi x}{L_x} \sin \frac{n\pi y}{L_y} \exp\left[-\left(\frac{K_x n^2 \pi^2}{L_x^2} + \frac{K_y j^2 \pi^2}{L_y^2}\right) t\right],$$

where K_x and K_y refer to thermal diffusivity components at the x and y directions; and the coefficient A_{nj} is given as

$$A_{nj} = \frac{4u_0}{nj\pi^2}[(-1)^n - 1][(-1)^j - 1].$$

In the present analysis, the numerical values adopted are $L_x = L_y = 3$, $K_x = K_y = 1.25$ and $u_0 = 30$. To solve for this problem we use a first order BEM to take the corners in the problem's domain into account. Table 2.5 shows a comparison of results for for a boundary discretization with 33

x	y	Exact [5]	$f = 1 + r$	$f = r^2 \log r$
2.4	1.5	1.065	1.1217	1.2053
2.4	2.4	0.626	0.6601	0.7299
1.8	1.5	1.723	1.8149	1.9210
1.8	1.8	1.639	1.7257	1.8172
1.5	1.5	1.812	1.9093	2.0256

Table 2.5: Interior Values for 1-BEM to equation $\nabla^2 u = \dot{u}$ at $t = 1.2$.

internal nodes and 24 boundary nodes, Figure 2.5 (Right), obtained with a

time step $\Delta t = 0.05$. It can be seen that the results seem to converge to values which are slightly higher than the exact ones.

Figure 2.6, shows the results for u at the centre point at each time-step. As expected in a thermal shock problem, the largest errors -an apparent
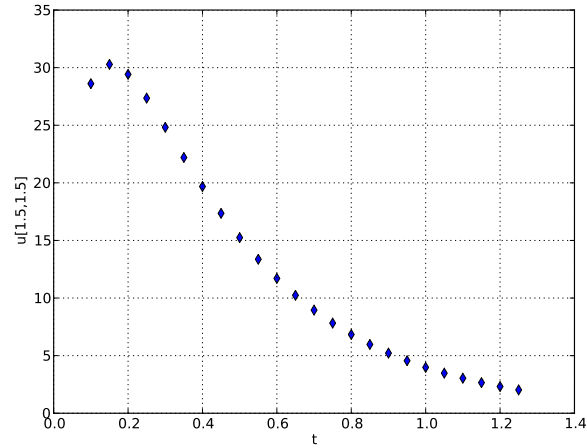
Figure 2.6: Central temperature response of a plate cooled by a boundary thermal shock.

increase in temperature- appear at the initial times since the shock is applied linearly over the first time step in the computational model and not suddenly as in the mathematical problem [18]. It can be observed, however, that the initial oscillations are quickly dampened.

Chapter 3

Transport in Porous Media

Interest by studying transport processes in porous rocks arise inside the oil industry. Several phenomena could be modelled using this type of processes. In a recovery process, a common oil-extracting operation, dilution or even loss of injected species can be expected as a consequence of heterogeneities in the medium. This irregularities gives place to fluid mixing. Two phenomena is identified in this transport processes: the molecular diffusion, a consequence of concentration gradients; and mechanical dispersion, a consequence of media heterogeneities. This is can be studied by considering the hydrodynamic dispersion: a combination of both previous mentioned effects. Thus, taking dispersive properties of porous media is relevant to the success of enhanced oil recovery projects.

Early studies considered analytical dispersion on tracer flow tests based on the convection-dispersion equation. These supposed dispersion coefficients as constants. This assumption, however, did not hold when operating at field tests because the dependence with the scale results fundamental. A model which solves the difficulties between different spatial scales is deduced from the stochastic form of the convection-dispersion equation and is given in this chapter. The resulting equation takes the form of a advective-diffusive transport equation with a time dependent diffusive parameter.

In this section of the Thesis, once the model is established, we use the DRMBEM tools developed in previous chapters to solve for a transport process with a time dependent dispersion term. We study numerical results for a particular case at the end of the chapter.

3.1   The Model

The relationship between concentration and dispersion coefficient was first gleaned from analytical solutions to the deterministic equations modelling recovery processes. These analytical dispersion models of tracer flow are based on the convection-dispersion equation and are restricted to cases of mixing governed by Fickian dispersion in one and two dimensional homogeneous media, Perkins [21]. These early models accounted, thus, for a constant dispersive parameter. The assumption of constant dispersion coefficients did not hold when operating at field inter-well scales because the scale of heterogeneity in the reservoir which is much larger than that in laboratory tests, Numbere and Erkal [16].

Reservoir heterogeneities increase the rate of solvent dispersion during tracer tests. Field measured dispersion coefficients were found to be space dependent and have been shown to vary approximately linearly with the scale of measurement, Gelhar [8]. As the flow paths become longer, greater variations of permeability are encompassed. Then, the correct prediction of fluid mixing and flow through heterogeneous porous media must integrate the effects of the many length scales of heterogeneity, Numbere and Erkal [16].

A stochastic approach is chosen, the model of the problem results form a geostatistical framework. This accounts for the uncertainty caused by limited reservoir data as well as the probabilistic distribution of reservoir heterogeneities. Considering only the heterogeneities caused by permeability variations, using a Monte-Carlo simulation technique, Warren and Skiba concluded that the mixing caused by macro-scale permeability variations can also be modelled using the conventional convection-dispersion equation. However, the space-dependent effective macroscopic dispersion coefficient should be used in place of the constant dispersion coefficient, Warren and Skiba [27].

Considering a small variance of the field's velocity, a weak heterogeneity in the media, assuming a constant viscosity and pressure gradient, Zhang deduces a dispersion coefficient, [29, 30]. The dispersion coefficient tensor contains three components, one for each spatial direction. For the unidirectional case we have

$$K(t) = \frac{q_m}{\bar{v}} \left(\frac{1}{1+\mu} \right) \left[\left(1 + \frac{\bar{v}t}{l} \right)^{1+\mu} - 1 \right].$$ (3.1)

Here μ is a fractal exponent which accounts for the model's multiple scales,

q_m is the variance of the velocity field, $\bar{v}$ is the mean velocity. As we can see, the effects of the porous media over the system are stated in the dispersion coefficient $K(t)$. At Figure 3.1 we see the behaviour of the dispersive
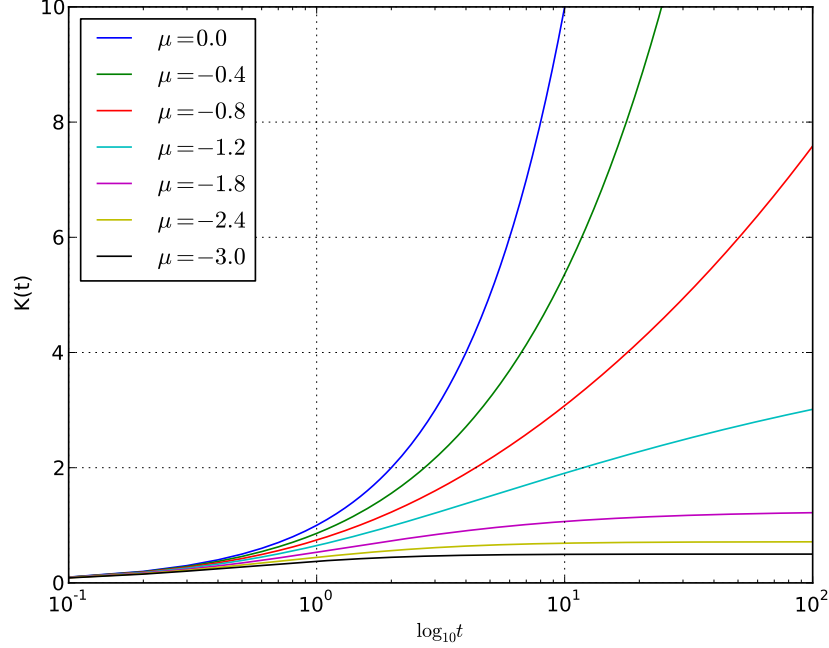
Figure 3.1: Evolution of dispersive coefficient for different fractal exponents

coefficient for different fractal exponents, K tends asymptotically to a constant value as μ decreases. As μ approaches zero, the dispersive coefficient growths more rapidly as time moves forward. This effects will be noted at the simulations presented in the next section.

The two dimensional form of the convection-dispersion equation with a space-dependent dispersion coefficient can be written as, Numbere and Erkal [16],

$$\frac{\partial u}{\partial t} = K(t) \left(\frac{\partial^2 u}{\partial x^2} + \frac{\partial^2 u}{\partial y^2} \right) - \bar{v} \frac{\partial u}{\partial x}. \tag{3.2}$$

where u is a concentration field referring to a single chemical specie, and $K(t)$ is given by, (3.1). This equation represents a transient isotropic dispersion with a unidirectional velocity profile.

3.2 The DRBEM for The Transport Equation

A dual reciprocity formulation of (3.2) follows the work of Patridge et. al [18], discussed at chapters 1 and 2. First, lets state equation (3.2) as,

$$K(t)\nabla^2 u = \left(\frac{\partial u}{\partial t} + \bar{v}\frac{\partial u}{\partial x}\right). \tag{3.3}$$

Experimental data proves that this equation describes the behaviour of a function u correctly describes the model presented, Numbere and Erkal [16]. Departing from this fact, existence of solutions to (3.3) is assumed. Then, assume that u is defined over Ω and the values of u are known at the domain's boundary Γ, $u|_\Gamma = \bar{u}$. This defines a Dirichlet problem over Ω. Comparing equation (3.3) with (2.2) we see that,

$$b(x, y, t) = \left(\frac{\partial u}{\partial t} + \bar{v}\frac{\partial u}{\partial x}\right). \tag{3.4}$$

Following the procedure defined on section 2.3, we start by defining N nodal points at Γ and L internal nodes at the interior of Ω. Then, one approximates the source term by a series of geometry-dependent functions

$$b(x, y, t) = \sum_{k=1}^{N+L} \alpha_k(t) f_k(x, y). \tag{3.5}$$

The approximating functions are defined so

$$\nabla^2 \hat{u}_k = f_k$$

can be solved for each f_k. Up next, we substitute (3.5) at (3.3)

$$\nabla^2 u = \frac{1}{K(t)} \sum_{k=1}^{N+L} \alpha_k(t) f_k(x, y). \tag{3.6}$$

Multiplying both sides of (3.6) by the fundamental solution to Laplace's equation and integrating over the domain yields

$$\int_\Omega (\nabla^2 u) u_i^* d\Omega = \frac{1}{K(t)} \sum_{k=1}^{N+L} \alpha_k(t) \int_\Omega (\nabla^2 \hat{u}_k) u_i^* d\Omega. \tag{3.7}$$

Note that the summation and the integral are interchanged by assuming smoothness. Using Green's second identity on both sides and approximating boundary integrals by summation over boundary elements gives for a source node $(x_i, y_i) \in \Omega$

$$\beta_i u_i + \int_\Gamma q_i^* u d\Gamma - \int_\Gamma u_i^* q d\Gamma =$$
$$\frac{1}{K} \sum_{k=1}^{N+L} \alpha_k \left(\beta_i \hat{u}_{ik} + \int_\Gamma q_i^* \hat{u}_k d\Gamma - \int_\Gamma u_i^* \hat{q}_k d\Gamma \right).$$

After the Boundary Element Method approximation over each boundary element we rewrite,

$$\beta_i u_i + \sum_{j=1}^{N} H_{ij} u_j - \sum_{j=1}^{N} G_{ij} q_j =$$
$$\frac{1}{K} \sum_{k=1}^{N+L} \alpha_k \left(\beta_i \hat{u}_{ik} + \sum_{j=1}^{N} H_{ij} \hat{u}_{jk} - \sum_{j=1}^{N} G_{ij} \hat{q}_{jk} \right). \quad (3.8)$$

The coefficient β_i takes a value of 1 if the node i is an interior point, 0.5 if it is on a smooth boundary, and a value given by the value if the angle at the corner otherwise. The definition of the known influence coefficients H_{ij} and G_{ij} depends on the election of constant element values or linear increments on u_j and q_j. After evaluation of the last equation at every nodal value we establish a $(N + L) \times (N + L)$ linear system

$$\mathbf{H}u - \mathbf{G}q = \frac{1}{K} \sum_{k=1}^{N+L} \alpha_j (\mathbf{H}\tilde{u}_k - \mathbf{G}\tilde{q}_k). \quad (3.9)$$

The α vector is defined to satisfy

$$\alpha = \mathbf{F}^{-1} \left(\frac{\partial u}{\partial t} + \bar{v} \frac{\partial u}{\partial x} \right). \quad (3.10)$$

Taking α into (3.9), and considering the expansion of the convective term, equation (2.38),

$$\mathbf{H}u - \mathbf{G}q = \frac{\mathbf{S}}{K} \left(\frac{\partial u}{\partial t} + \bar{v} \frac{\partial \mathbf{F}}{\partial x} \mathbf{F}^{-1} u \right), \quad (3.11)$$

where

$$\mathbf{S} = (\mathbf{H}\tilde{\mathbf{U}} - \mathbf{G}\tilde{\mathbf{Q}})\mathbf{F}^{-1}.$$

By defining

$$\mathbf{C} = -\frac{\mathbf{S}}{K}, \quad \mathbf{R} = \frac{\mathbf{S}}{K}\left(\bar{v}\frac{\partial\mathbf{F}}{\partial x}\mathbf{F}^{-1}\right),$$

one can rewrite (3.11) as

$$\mathbf{C}\dot{\mathbf{u}} + (\mathbf{H} - \mathbf{R})\mathbf{u} = \mathbf{G}\mathbf{q}. \tag{3.12}$$

Equation (3.12) is solved with a discrete time-marching procedure. A linear approximation is used for the variation of u and q within each time step, *i.e.*,

$$u = (1 - \theta_u)u^m + \theta_u u^{m+1}, \tag{3.13}$$

$$q = (1 - \theta_q)q^m + \theta_q q^{m+1}, \tag{3.14}$$

$$\dot{u} = \frac{1}{\Delta t}(u^{m+1} - u^m). \tag{3.15}$$

Substituting equations (3.13)-(3.15) into equation (3.12) produces

$$\left[\frac{1}{\Delta t}\mathbf{C} + \theta_u(\mathbf{H} - \mathbf{R})\right]\mathbf{u}^{m+1} - \theta_q\mathbf{G}\mathbf{q}^{m+1} =$$

$$\left[\frac{1}{\Delta t}\mathbf{C} + (1 - \theta_u)(\mathbf{H} - \mathbf{R})\right]\mathbf{u}^m - (1 - \theta_q)\mathbf{G}\mathbf{q}^m \tag{3.16}$$

The right side of equation (3.16) is a known vector at all times. It uses the initial values specified at $t = 0$ and is calculated in subsequent time steps. At each time step the linear system (3.16) is reduced and solved for the unknown values of u and q.

The ADT equation on a square plate.

The performance of the numerical method has been proved over the discussion of previous examples. Now we will study some particular cases for the advective-dispersive transport equation.

The problem of advective-dispersive transport in a square plate is presented. For this particular case we set the problem's domain as a square plate Ω. The initial condition corresponds to $u_0 = 0$ over Ω. Let the unit square

have a Dirichlet boundary condition $\bar{u} = 0$ everywhere except at $x = 0$, where the condition is $\bar{u} = 300$ for $0 < y < 3$, Figure 3.2,

$$\bar{u} = \begin{cases} 0, & y = 3, \quad 0 < x < 3 \\ 0, & y = 0, \quad 0 < x < 3 \\ 0, & x = 3, \quad 0 < y < 3 \\ 300, & x = 0, \quad 0 < y < 3 \end{cases}$$

The boundary condition remains fixed for every t.
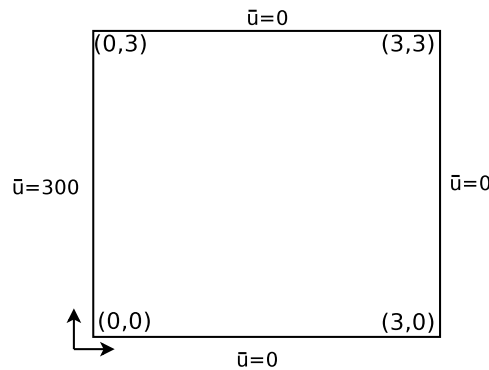
Figure 3.2: Boundary conditions for advective-dispersive transport problem

μ	$f = 1 + r$
0	129.7129
-0.4	133.5025
-0.8	137.4781
-1.8	148.0798
-3	161.5357

Table 3.1: u evaluated at $[1.5, 1.5]$, $t = 1.2$

To obtain solution for this problem we use a first order BEM to take corners into account. Solving this problem we defined a boundary discretization of 24 straight elements and 100 interior nodes, Figure 3.3. The problem was solved using the radial basis functions $f = 1 + r$. The values of μ where taken as $-3 \leq \mu \leq 0$, accordingly with Figure 3.1. Concentration profiles for the central point of the plate are presented at Figure 3.4. Full plate profiles for different times are presented at Figures 3.5 to 3.8. At the figures we can see
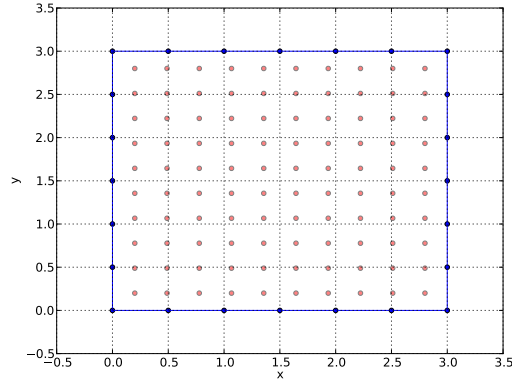
Figure 3.3: Domain discretization for advective-dispersive transport problem

that a variation over the fractal exponent implies a slightly different profile evolution. This issue needs to be taken with precaution in field operation.
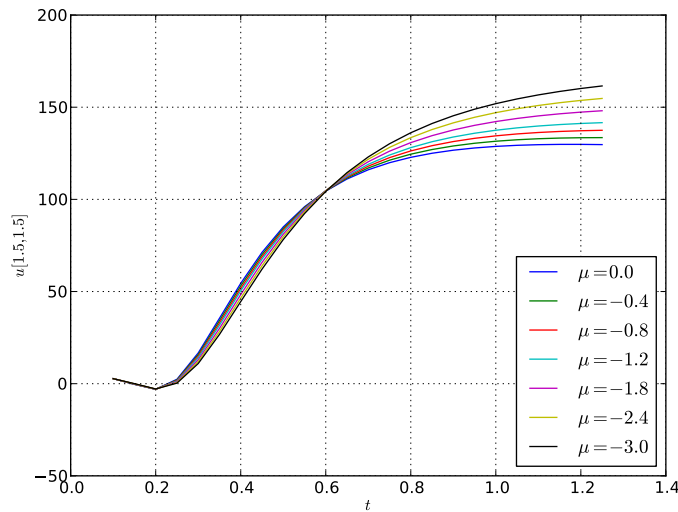
Figure 3.4: Concentration profile evolution for the plate at $[1.5, 1.5]$ for different values of μ.

Apparently, decrements over the fractal parameter μ imply an increment on the concentration at $t = 1.2$. Table 3.1 shows a comparison of results

for the concentration profile u at the center of the plate for $t = 1.2$ using different values for β.

This behaviour can somehow be interpreted using the problem's model: If we analyse the dispersion coefficient we see that as the fractal coefficient takes smaller values, the growth of the dispersive parameter is decreasing. This implies a slowest movement of the chemical species in Ω, implying a mayor accumulation. This fact can also be taken as the cause for the profile evolution at Figures 3.5 to 3.8. So, the model, considering a temporal dependent dispersive coefficient, predicted correctly behaviour that does not result obvious at first glance.
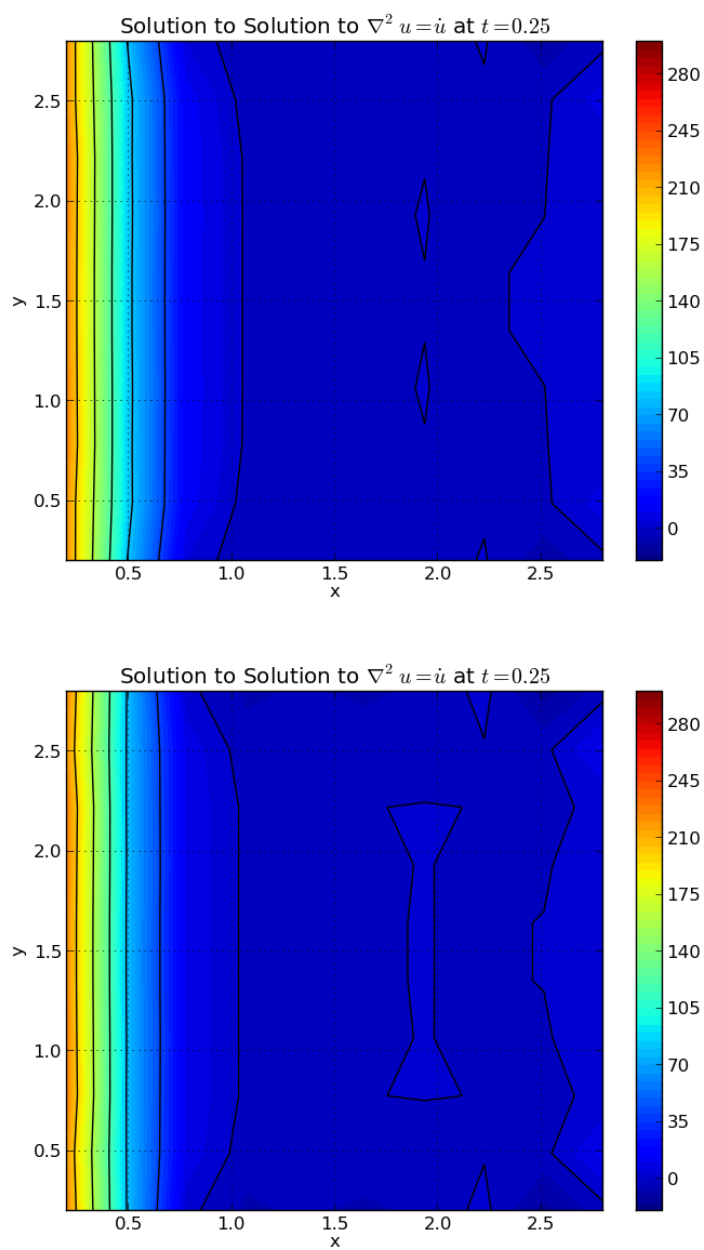
Figure 3.5: Concentration profile for the plate at $t = 0.25$ for: $\mu = 0$, up; $\mu = -3.0$, down.
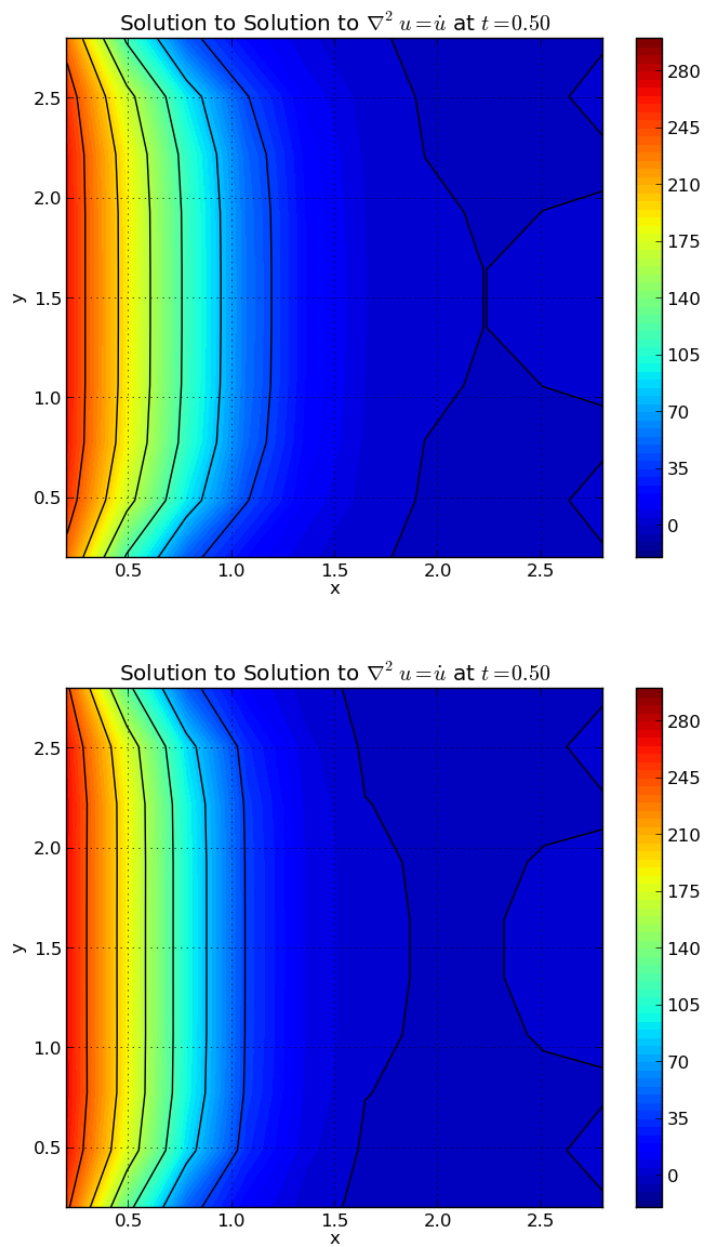
Figure 3.6: Concentration profile for the plate at $t = 0.50$ for: $\mu = 0$, up; $\mu = -3.0$, down.
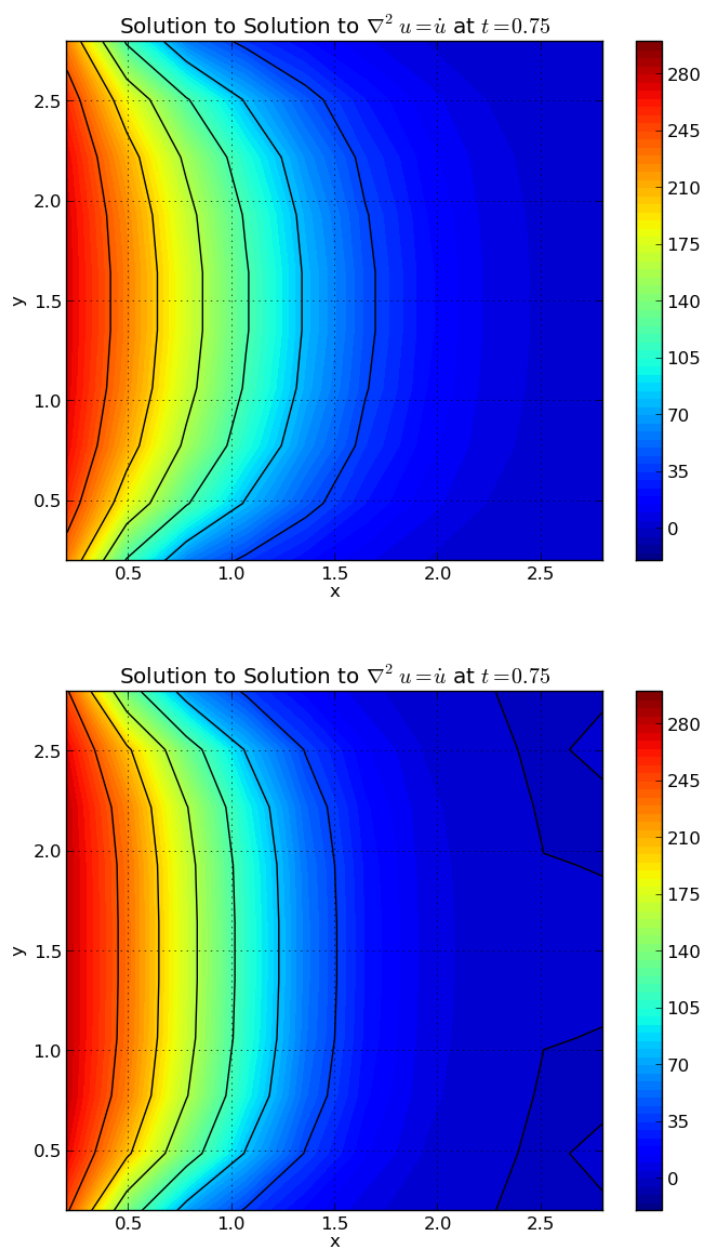
Figure 3.7: Concentration profile for the plate at $t = 1.00$ for: $\mu = 0$, up; $\mu = -3.0$, down.
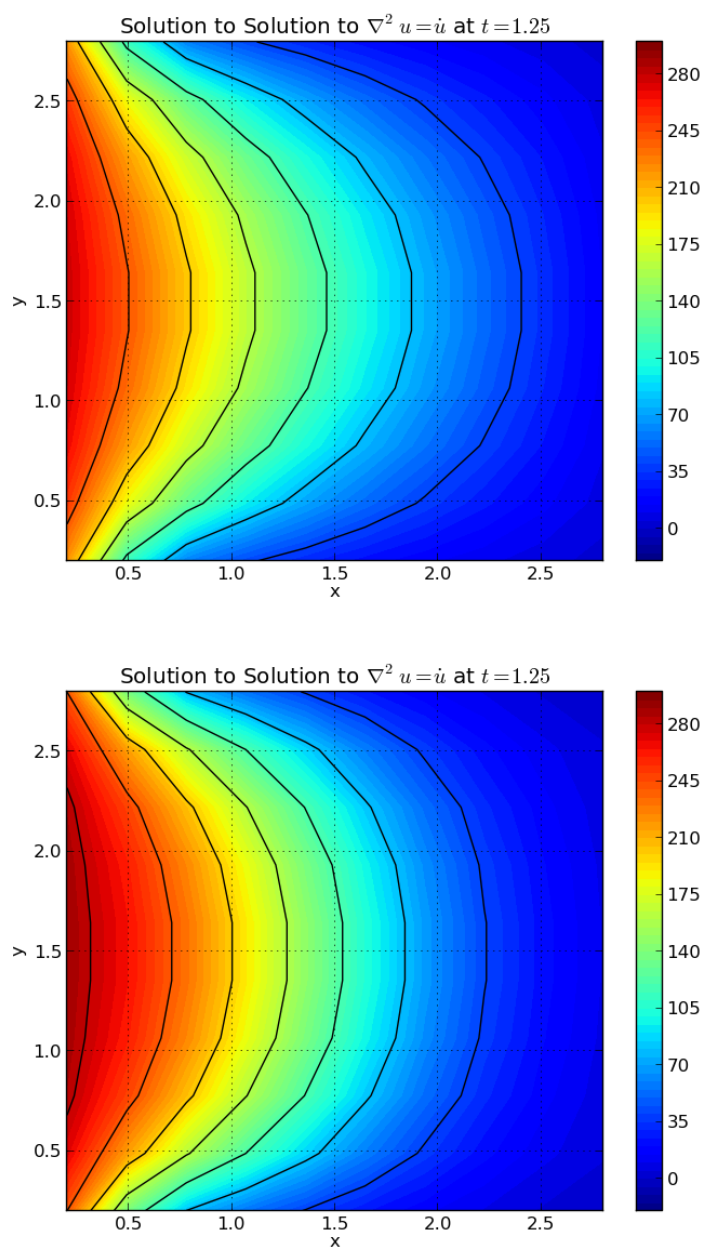
Figure 3.8: Concentration profile for the plate at $t = 1.25$ for: $\mu = 0$, up; $\mu = -3.0$, down.

Chapter 4

Conclusions

Boundary element methods constitute a useful tool for studying models described by elliptical PDE's over regular or irregular domains. The main advantage of BEM against other class of numerical methods corresponds to the easiness of its implementation, and the flexibility of the method. The main disadvantage of the BEM resides on the need of knowing some Green's function related to the problem's model, which is not always available. From the examples discussed we verify that the method approximates the solution to Laplace's equation for different boundary conditions. As for the results there exists not much difference between the application of a zero order and a first order boundary element method for smooth boundaries. For boundaries which contains cusps, however, there is a slightly improvement by using a first order BEM because it takes into account non-smooth boundary-points.

Even considering that the foundation of BEM relies on Laplace's equation, is possible to extend its theoretical basis in order to solve more complex equations. As noted in Chapter 2, using Laplace's fundamental solution we enable a boundary solution, which was not available at first instance, for Poisson's problems -where the source term could even include the potential or time dependent terms-. The extension of fundamental solutions gives us a flexible method which, departing from a simple equation, can be easily extended to solve a broader class of problems. In this sense, boundary element methods result in a interesting tool which deserves more study and developement.

In this thesis we used Laplace's fundamental solution to construct a boundary element method to solve boundary value problems. The use of Laplace's fundamental solution restricts the method's accuracy because of

the approximations in the source term made by BEM. Future work could include a comparative in the implementation of boundary element methods using different fundamental solutions. Fundamental solutions to Helmholtz and advective transport equations are available. Particularly, an approach to deal with time-dependent terms using fundamental solutions could be developed. Both issues are presented by Pozrikidis at [22].

Also, a comparative study between a wider spectrum of basis functions is suggested as a starting point for future investigation. Different interpolating functions gives different convergence on the method, resulting on more or less precise results.

Refinement of the method is also necessary for future implementation. At this point we build a boundary element method with linear approximations and straight boundary elements. Depending on the future course of work, quadratic or cubic elements must be deployed in the method to improve precision in results.

Finally, a dispersive-advective transport process was solved. Once the implementation of the method was developed, we see that the process to apply the DRBEM to the model follows easily, even with the time dependent terms. With a relatively small amount of data -boundary and initial conditions at a few domain points- the numerical method can predict the behaviour of the problem. Even considerable concentration differences were predicted by the model due to its fractal approach over the problems heterogeneities.

As a final conclusion we can present the boundary element formulation as an effective, flexible tool, which can be easily extended from simple problems -Laplace's Equation- to a little more complicated -Dispersive-advective transport equation-, and other kind of partial differential equations. This thesis has showed the development and implementation of the numerical method to solve boundary valued problems in future implementations.

List of Figures

List of Tables

Bibliography

[1] R.B. Bird, W.E. Stewart, and E.N. Lightfoot. *Transport Phenomena.* Wiley International edition. Wiley, 2006.

[2] C. A. Brebbia, J. C. Telles, Faria, and L. C. Wrobel. *Boundary element techniques: theory and applications in engineering*, volume 5. Springer-Verlag Berlin, 1984.

[3] C.A. Brebbia. *Recent advances in boundary element methods.* Pentech Press, 1978.

[4] C.A. Brebbia. *The boundary element method for engineers.* Pentech Press, 1984.

[5] J.C. Bruch and G. Zyvoloski. Transient two-dimensional heat conduction problems solved by the finite element method. *International Journal for Numerical Methods in Engineering*, 8(3):481–494, 1974.

[6] D.J. Danson, C.A. Brebbia, and R.A. Adey. Beasy a boundary element analysis system. In R.A. Adey, editor, *Engineering Software III*, pages 254–271. Springer Berlin Heidelberg, 1983.

[7] K.O. Dimon. *Foundations of Potential Theory.* Lightning Source Incorporated, 2007.

[8] L. W. Gelhar. Stochastic subsurface hydrology from theory to applications. *Water Resources Research*, 22(9S):135S–145S, 1986.

[9] M.A. Golberg and C.S. Chen. The theory of radial basis functions applied to the bem for inhomogeneous partial differential equations. *Boundary Elements Communications*, 5(2):57–61, 1994.

[10] M.A. Golberg and C.S. Chen. A bibliography on radial basis function approximation. *Boundary Elements Communications*, 7:155–163, 1996.

[11] MA Golberg, CS Chen, H Bowman, and H Power. Some comments on the use of radial basis functions in the dual reciprocity method. *Computational Mechanics*, 21(2):141–148, 1998.

[12] P. M. Gresho and R. L. Lee. Don't suppress the wiggles—they're telling you something! *Computers & Fluids*, 9(2):223–253, 1981.

[13] M.A. Jaswon. Integral equation methods in potential theory. i.

[14] J.D. Logan. *Applied mathematics*. Wiley-Interscience publication. Wiley, 1997.

[15] D. Nardini and C.A. Brebbia. A new approach to free vibration analysis using boundary elements. *Applied mathematical modelling*, 7(3):157–162, 1983.

[16] D.T. Numbere and A. Erkal. A model for tracer flow in heterogeneous porous media. In *SPE Asia Pacific Conference on Integrated Modelling for Asset Management, Kuala Lumpur, Malaysia*, pages 37–44. Society of Petroleum Engineers International, Inc, March 1998.

[17] J.T. Oden and J.N. Reddy. *An introduction to the mathematical theory of finite elements*. Pure and applied mathematics. Wiley, 1976.

[18] P.W. Partridge, C.A. Brebbia, and L.C. Wrobel. *The dual reciprocity boundary element method*. International series on computational engineering. Computational Mechanics Publications, 1992.

[19] G. Payre, M. De Broissia, and J. Bazinet. An 'upwind'finite element method via numerical intergration. *International Journal for Numerical Methods in Engineering*, 18(3):381–396, 1982.

[20] F. Periago. A first step towards variational methods in engineering. *International Journal of Mathematical Education in Science and Technology*, 34(4):549–559, 2003.

[21] T.K. Perkins and O.C. Johnston. A review of diffusion and dispersion in porous media. *SPE Journal*, 3(2), 1963.

[22] C. Pozrikidis. *A Practical Guide to Boundary Element Methods with the Software Library BEMLIB*. Taylor & Francis, 2002.

[23] D. Rainville and P.E. Bedient. *Elementary Differential Equations*. Collier-Macmillan International Editions, 1969.

[24] W.A. Strauss. *Partial Differential Equations, Student Solutions Manual: An Introduction*. John Wiley & Sons, 2008.

[25] G.T. Symm. Integral equation methods in potential theory. ii.

[26] David von Seggern (University of Nevada-Reno). Laplace's equation on a square from the wolfram demonstrations project, 2013.

[27] J. Warren and F. Skiba. Macroscopic dispersion. *Old SPE Journal*, 4(3):215–230, 1964.

[28] L.C. Wrobel, C.A. Brebbia, and D. Nardini. The dual reciprocity boundary element formulation for transient heat conduction. *Finite Elements in Water Resources VI*, 1986.

[29] Q. Zhang. Length scales, multi-fractals and non-fickian diffusion. *Computational Methods in Water Resources IX*, 2:59–70, 1992.

[30] Q. Zhang. A multi-length-scale theory of the anomalous mixing-length growth for tracer flow in heterogeneous porous media. *Journal of Statistical Physics*, 66(1-2):485–501, 1992.